ACCEPTED VERSION

Jolly, Lachlan Andrew; Homan, Claire Christine; Jacob, Reuben; Barry, Simon Charles; Gecz, Jozef, *The UPF3B gene, implicated in intellectual disability, autism, ADHD and childhood onset schizophrenia regulates neural progenitor cell behaviour and neuronal outgrowth*, Human Molecular Genetics, 2013; 22(23):4673-4687

COPYRIGHT STATEMENT

This is a pre-copy-editing, author-produced PDF of an article accepted for publication in Human Molecular Genetics *ollowing peer review. The definitive publisher-authenticated version* Jolly, Lachlan Andrew; Homan, Claire Christine; Jacob, Reuben; Barry, Simon Charles; Gecz, Jozef, *The UPF3B gene, implicated in intellectual disability, autism, ADHD and childhood onset schizophrenia regulates neural progenitor cell behaviour and neuronal outgrowth*, Human Molecular Genetics, 2013; 22(23):4673-4687 *is available online at:*
http://hmg.oxfordjournals.org/content/22/23/4673

PERMISSIONS

http://www.oxfordjournals.org/access_purchase/self-archiving_policyb.html

Author Self-Archiving Policy

- Authors may upload their accepted manuscript PDF ("a post-print*") to institutional and/or centrally organized repositories, but must stipulate that public availability be delayed until **12 months after first online publication** in the journal. Please note that a special policy applies for articles published under the *Oxford Open* initiative (see below).

15 July 2014

http://hdl.handle.net/2440/81741

HMG Advance Access published July 2, 2013

The *UPF3B* Gene, Implicated in Intellectual Disability, Autism, ADHD and Childhood Onset Schizophrenia Regulates Neural Progenitor Cell Behaviour and Neuronal Outgrowth

Lachlan A. Jolly[1,2], Claire Homan[1,2], Reuben Jacob[3], Simon Barry[2] and Jozef Gecz[*,1,2,3]

[1]Department of Genetic and Molecular Pathology, SA Pathology, North Adelaide, 5006, Australia
[2]School of Paediatrics and Reproductive Health, The University of Adelaide, Adelaide, 5000, Australia
[3]School of Molecular and Biomedical Science, The University of Adelaide, Adelaide, 5000, Australia
[*]Corresponding Author: Jozef Gecz: Department of Genetic and Molecular Pathology, SA Pathology at the Women's and Children's Hospital, North Adelaide, SA 5006, Australia. jozef.gecz@adelaide.edu.au, Tel: +61 8 8161 6339, Fax: +61 8 8161 7342

Downloaded from http://hmg.oxfordjournals.org/ at University of Adelaide on July 3, 2013

© The Author 2013. Published by Oxford University Press. All rights reserved.
For Permissions, please email: journals.permissions@oup.com

ABSTRACT

Loss of function mutations in *UPF3B* result in variable clinical presentations including intellectual disability (ID, syndromic and non-syndromic), autism, childhood onset schizophrenia and attention deficit hyperactivity disorder. UPF3B is a core member of the nonsense mediated mRNA decay (NMD) pathway that functions to rapidly degrade transcripts with premature termination codons (PTCs). Traditionally identified in thousands of human diseases, PTCs were recently also found to be part of 'normal' genetic variation in human populations. Furthermore, many human transcripts have naturally occurring regulatory features compatible with 'endogenous' PTCs strongly suggesting roles of NMD beyond PTC mRNA control. In this study, we investigated the role of Upf3b and NMD in neural cells. We provide evidence that suggests Upf3b dependent NMD (Upf3b-NMD) is regulated at multiple levels during development including regulation of expression and sub-cellular localisation of Upf3b. Furthermore complementary expression of Upf3b, Upf3a and Stau1 stratify the developing dorsal telencephalon, suggesting that alternative NMD, and the related Staufen1 mediated mRNA decay (SMD) pathways are differentially employed. Loss of Upf3b-NMD in neural progenitor cells resulted in the expansion of cell numbers at the expense of their differentiation. In primary hippocampal neurons loss of Upf3b-NMD resulted in subtle neurite growth effects. Our data suggest that the cellular consequences of loss of Upf3b-NMD can be explained in-part by changes in expression of key NMD-feature containing transcripts which are commonly deregulated also in patients with *UPF3B* mutations. Our research identifies novel pathological mechanisms of *UPF3B* mutations and at least partly explains the clinical phenotype of *UPF3B* patients.

Downloaded from http://hmg.oxfordjournals.org/ at University of Adelaide on July 3, 2013

INTRODUCTION.

Intellectual disability (ID) is estimated to affect ~2% of the world's population. This vast collection of clinically variable and genetically heterogeneous disorders of the brain is primarily characterised by compromised ability to learn and remember. Socio-economic impact of ID is considerable (1, 2). There are currently over 380 genes and hundreds of other loci in which mutations (or copy number variations; CNVs) are reported to cause ID (1). An estimated 10-15% of ID genes are on the X-chromosome, also known as X-linked ID (XLID) (3). Whilst the identification of the full spectrum of genetic causes of ID remains a major challenge, better understanding of the molecular pathways underlying ID is becoming imminent.

Mutations in the *UPF3B* gene have been identified to cause XLID (MIM: 300676). To date about 10 separate families with *UPF3B* mutations, including missense, frameshift and nonsense mutation, all of which result in a loss of *UPF3B* function, are known (4-8). In addition to ID, *UPF3B* patients also present with attention-deficit hyperactivity disorder (6, 7), autism (4, 5, 7) and schizophrenia (7). The severity and type of clinical presentations also vary, within and between families (4-6). These and molecular, whole transcriptome, analysis of UPF3B patient cells, suggest that UPF3B protein is crucial for normal development and function of the brain (9). What is the underlying molecular mechanism remains largely unknown.

UPF3B is a member of the exon-junction complex (EJC) that is essential for NMD function. NMD's primarily role is to degrade transcripts with premature termination codons, thereby protecting the cell against translation of truncated proteins with potentially deleterious effect (10). Following pre-mRNA splicing, UPF3B remains associated with

Downloaded from http://hmg.oxfordjournals.org/ at University of Adelaide on July 3, 2013

nascent mRNA at exon-exon boundaries (11, 12). Subsequently, during nuclear export of mRNA, UPF3B becomes bound by a second core NMD factor UPF2 (11, 12). During the pioneer round of translation, the ribosome usually removes EJC complexes. That most mammalian genes harbour their normal termination codon within their last exon has been exploited by the NMD machinery to identify PTC-containing transcripts, whereby the unusual deposition of an exon-junction complex downstream of a termination codon becomes an NMD triggering feature (10). Ribosome stalling at a PTC triggers sequential generation of an active NMD complex by recruiting the third core, and critically required, NMD factor UPF1 via interaction with UPF2 (10, 13). Once bound, UPF1 serves this complex by directing targeted degradation of the mRNA through its ATPase RNA helicase activity and various interactions with ribonucleases (10, 13-16).

NMD is now recognised as an important regulator of the transcriptome, with 'PTCs' serving as a natural regulatory feature. These endogenous PTCs can occur as a result of alternative splicing events, the presence of an upstream open reading frame (uORF), or where an exon-exon boundary is present or introduced in the 3'untranslated region (UTR). In addition, 3'UTRs >1.5 Kb can also trigger NMD (10). Loss of NMD factor function was shown to lead to deregulation of ~5% of the transcriptome across different cell types and animal models (9, 17-23). NMD function is crucial for embryonic development, with *Upf1* and *Upf2* knockout mice displaying embryonic lethality (4, 21, 24).

Whilst UPF1 is essential for NMD, alternative pathways acting independently of UPF3B and UPF2 exist (17, 25). This has been demonstrated in patients with *UPF3B* PTC mutations, where the PTC mRNA of *UPF3B* is itself NMD degraded in the absence of the UPF3B protein (4, 9). In *UPF3B* patient cells, the activity of the alternative pathway involving

Downloaded from http://hmg.oxfordjournals.org/ at University of Adelaide on July 3, 2013

UPF3B paralog, *UPF3A,* appears critical for the patient's clinical outcome. In the absence of UPF3B, variable stabilisation of UPF3A occurs, which inversely correlates with the clinical severity of the neurological features of the patients (9, 18). Transcriptome profiling of UPF3B deficient human cells supports the idea that the level of activity of the UPF3A dependent NMD (UPF3A-NMD) pathway can partially rescue the loss of UPF3B-NMD function (9) . In addition to the alternative UPF3A pathway, it has been established that NMD pathways are influenced by the competitive strength of the *Staufen1* mediated mRNA Decay (SMD) pathway (26, 27). SMD involves the mRNA binding protein Staufen1 (STAU1), which binds cognate sequences in the 3'UTR of target transcripts (Stau1 binding sites; SBS), and recruits the mRNA decay machinery via an interaction with UPF1 (28, 29). As UPF1 binding to UPF2 or STAU1 is mutually exclusive, a competitive balance between NMD and SMD exists, whereby one pathway assumes dominance (26, 27). Importantly, this balance is functionally required during cell processes like those of myoblast maintenance and differentiation (26). Thus in any cell, including those present during brain development, the relative contribution of *UPF3B* function may be influenced also by the activity of the partially redundant UPF3A-NMD pathway, and by the competitive SMD pathway (18, 27).

It has also emerged that nervous system development and function is sensitive to NMD function. In addition to the evidence provided by study of the *UPF3B* patients, experiments in mice revealed that haploinsufficiency of the accessory NMD factor *Magoh* results in microcephaly (30). Knock-down of NMD factors in zebrafish resulted in brain growth and patterning defects, whilst in fly, hemizygous deletion of *Upf1* or the accessory factors *Smg1* and *Smg6* disrupted synapse structure and function (31, 32). Other studies have identified that NMD of key transcripts is required for essential neuronal functions

Downloaded from http://hmg.oxfordjournals.org/ at University of Adelaide on July 3, 2013

including activation of global brain specific splicing programs, neurite growth, synaptogenesis and synaptic strength (9, 33-36).

Thus far, we approached the identification of key pathological mechanisms in *UPF3B* patients by interrogating the transcriptomes of patients' lymphoblastoid cell lines (LCLs) (9). In these cells, loss of UPF3B-NMD resulted in deregulation of ~5% of the LCL transcriptome, including several genes with defined roles in the development of the brain. In this study, we first reveal the complex regulation of Upf3b expression during brain development that involves both gene expression and subcellular localisation of Upf3b itself. Upf3b expression is complemented by the expression of alternative NMD and competitive SMD pathway factors, suggesting a balancing of respective pathway activity. We show in neural progenitor cells (NPCs), that loss of Upf3b-NMD promoted self-renewal whilst delaying differentiation. Upf3b-NMD was also required in post-mitotic neurons, where it was involved in regulating neurite growth. In both cell types, loss of Upf3b-NMD altered the expression of key NMD feature containing transcripts, including *Six3* in NPCs, and *Nrcam* and *Robo1* in neuronal cells, which could help explain the cellular alterations, and which were also deregulated in human patient cells. Our results provide cellular and molecular evidence of the role of *Upf3b*-NMD during brain development and identify likely pathological mechanisms underpinning *UPF3B*-related neurological phenotypes.

Downloaded from http://hmg.oxfordjournals.org/ at University of Adelaide on July 3, 2013

RESULTS

Upf3b is expressed during brain development

We initially set out to identify the stages, events and cell types of brain development that are potentially sensitive to Upf3b-NMD function. It is well established that Upf3b functions in a partially redundant fashion with Upf3a, and that the NMD pathways are in a competitive functional balance with the SMD pathway (9, 17, 18, 26, 27). In view of these findings, we considered sensitivity to Upf3b-NMD activity would be a product of (1) *Upf3b* expression itself, (2) expression of *Upf3a*, and (3) activity of the SMD pathway as reported by the expression of the key SMD factor *Stau1*. We first employed qRT-PCR to identify temporal expression profiles of these genes during brain development. All three genes were expressed in the brain from an early time point of embryonic day 10.5 (E10.5) through to adulthood, with *Upf3b* and *Stau1* showing comparable trends and levels, >10 fold above that of *Upf3a* **(Supplementary Figure 1)**. Next we used *in-situ* hybridisation to reveal the spatial distribution of mRNA expression of these genes **(Supplementary Figure 2)**. At E10.5, *Upf3b* was broadly expressed in most tissues, but particularly strong in the developing central nervous system (CNS). At E14.5, a restriction in *Upf3b* expression within the CNS was revealed; in the forebrain, *Upf3b* was found highly enriched in the NPCs resident within the ventricular zones, which was maintained at E18.5 **(Supplementary Figure 2 and Figure1)**. At E18.5 and beyond, *Upf3b* transcripts were detected in the neurons of the cortical plate and adult cortical layers, and were highly expressed in the stratum pyramidale and dentate gyrus structures of the hippocampus **(Supplementary Figure 2 and 3)**. As in the forebrain NPCs, *Upf3b* mRNA was also highly expressed in the granule cell progenitors within the external germinal layer of the developing cerebellum, and also later in the neurons of the

Downloaded from http://hmg.oxfordjournals.org/ at University of Adelaide on July 3, 2013

adult structure **(Supplementary Figure 2 and 4)**. In comparison, the spatial distribution of *Stau1* transcripts was similar to *Upf3b*, whilst *Upf3a* transcripts were found broadly across all CNS structures **(Supplementary Figure 2-4)**.

Upf3b expression and localisation is dynamic during cortical development

We extended our study to include analysis of Upf3b protein expression. For this we used our well established in-house antibody (4, 9), which we further validated using mouse lysates **(Supplementary Figure 5).** We compared Upf3b protein expression with mRNA expression, and expression of other NMD and SMD factors. Initially we investigated the E14.5 dorsal telencephalon, the peak neurogenic phase of cortical development **(Figure 1 A)**. We observed a discontinuity between *Upf3b* mRNA and protein expression; whilst mRNA was highly enriched in the ventricular zone, protein was more highly expressed in the cortical plate. This discontinuity was not observed at later time points of cortical development. In contrast, the protein distribution of Upf3a and Stau1 correlated with their respective mRNA spatial distributions such that Upf3a was expressed at low levels across the developing telencephalic wall, and Stau1 was enriched within the ventricular zone, as was Upf1. Thus it was apparent that the E14.5 embryonic forebrain could be divided based on the expression of NMD and SMD factors; high Upf1 and Stau1 expression demarcating the ventricular zone, whilst high Upf3b expression demarcating the cortical plate **(Figure 1 A)**. The heterogeneous expression profiles of Upf3b, Upf3a and Stau1 became even more dynamic and complex later during cortical development, with each displaying predominant enrichment within various cell populations and layers of the developing cortex **(Supplementary Figure 6)**. Next we focussed specifically on Upf3b expression across embryonic stages of cortical

Downloaded from http://hmg.oxfordjournals.org/ at University of Adelaide on July 3, 2013

development, E10.5-E18.5 **(Figure 1 B)**. These studies revealed differential subcellular localisations, both within and across developmental stages. In the ventricular zones at E10.5 and E14.5, Upf3b was predominantly excluded from nuclear regions of NPCs, whilst in NPCs of the ventricular zone at E18.5, and in most neurons of the cortical plate structures (at E14.5 and E18.5), Upf3b displayed prominent nuclear localisation **(Figure 1 B and Supplementary Figure 7)**. Both the mRNA-protein discontinuity and the differential nuclear localisation phenomena of Upf3b were also observed using an *in-vitro* step-wise differentiation of neurons from murine embryonic stem cells **(Supplementary Figure 8).** Finally, we compared the amount of Upf3b expressed in both ventricular zone and cortical plate cells using established quantitative microscopy techniques. Expression within ventricular zones was comparable between E10.5 and E14.5, but 1.6 fold higher at E18.5, and 2-3 fold higher in the cortical plates at E14.5 and 18.5 **(Supplementary Figure8)**. Together these data suggest that *Upf3b* expression is complex during cortical development, but tended to be higher and more nuclear localised in cells of more advanced differentiation status.

Upf3b is highly expressed in hippocampal neurons

As our *in-situ* data revealed high mRNA expression of *Upf3b* within the hippocampus **(Supplementary Figure 2 and 3)**, this warranted further investigation. We isolated these cells and allowed them to grow *in vitro*, a process which mimics their *in-vivo* growth and maturation (37). During this growth, *Upf3b* mRNA expression increased **(Figure 2 A)**. Because Upf3b is localised throughout neurons, including synapses (5), we asked whether *Upf3b* expression might be regulated by neuronal activity, a feature displayed by many

Downloaded from http://hmg.oxfordjournals.org/ at University of Adelaide on July 3, 2013

synaptically functioning proteins. Upon chronic depolarisation of *in-vitro* cultured hippocampal neurons using 55mM KCl treatment (38), we observed a reduction in the level of *Upf3b* mRNA after 2 hours **(Figure 2 B)**. Thus *Upf3b* transcription was dynamic during both neuronal growth and in response to synaptic activity. Next, we employed immunohistochemistry to reveal *in-situ* protein expression and localisation of Upf3b, together with Upf3a and Stau1. Upf3b was localised throughout the cell, but enriched in the cell body and nucleus. In contrast, Stau1 was evenly distributed throughout the cell, whilst Upf3a displayed exclusion from nuclei **(Figure 2 C)**. Similar results were observed for cortical neurons, whilst expression of all three factors was collectively enriched, and similarly distributed, within Purkinje cells of the cerebellum **(Supplementary Figure 10 and 11)**. Together, these data confirm the high expression of *Upf3b* in mature neurons, including hippocampal neurons, and further suggests that the predominant subcellular distribution of Upf3b, Upf3a and Stau1 is regulated in a cell-type specific manner.

Loss of Upf3b function promotes NPC self-renewal.

Because *Upf3b* was highly expressed in the ventricular zone at E18.5 of the developing cortex, we enquired whether it was required for aspects of NPC biology, namely their ability to self-renew and differentiate. To stably reduce *Upf3b* expression in these cells we screened shRNA sequences for their ability to knock-down *Upf3b*. We identified 5 shRNA sequences that efficiently knocked *Upf3b* expression down in mouse NIH3T3 fibroblast cells **(Supplementary Figure 12)**. We then isolated NPCs from the E18.5 cortex and grew them non-adherently as neurospheres (39). Following a brief expansion, we transduced NPCs with lentiviral particles delivering a transfer vector that constitutively expressed GFP and either

Downloaded from http://hmg.oxfordjournals.org/ at University of Adelaide on July 3, 2013

control shRNAs (targeted against luciferase (Luc) , a scrambled *Upf3b* specific sequence (S2)) or shRNAs that target *Upf3b* (T2, T5 or a mixture of both T^{2+5}). Following transduction, GFP positive cells were isolated by Fluorescent Activated Cell Sorting (FACS) to produce pure populations of transduced cells. These cells remained greater than 95% GFP positive even after 7 passages, suggesting stable delivery of the shRNA (data not shown). For the following sets of experiments, we compared pooled results from control cell lines (Wild-type (WT; un-transduced), Luc and S2) with Upf3b-shRNA cell lines (T2, T5 and T2+5), to control for both the effects of viral transduction and shRNA off-target effects. On average, delivery of *Upf3b* shRNA reduced the *Upf3b* mRNA by ~2-fold, however the protein levels of Upf3b were reduced by 88% **(Supplementary Figure 13 and Figure 3 A and B)**. To determine whether the loss of Upf3b in NPCs impaired Upf3b-NMD, we analysed the mRNA of well established target genes *Atf4*, *Snord* and *Gas5,* which are commonly referenced in the literature to report on the activity Upf3b-NMD (17, 19, 21, 40). The reduction of Upf3b resulted in increased expression of the *Snord* and *Atf4* transcripts, suggesting that the Upf3b-NMD pathway had indeed been compromised **(Figure 3 C)**. Using an enzyme based proliferation assay we observed a significant proliferative advantage in NPCs lacking Upf3b when grown as neurospheres at low (i.e. clonal) density. They exhibited a 1.6- and 1.4-fold increase in growth over controls at days 3 and 6 of culture respectively **(Figure 3 D)**. This reduction might be explained by (1) an increased reduced percentage of proliferative cells, (2) a shortened cell cycle length or (3) an increased in number of sphere forming cells and thus sphere forming capacity . We used EdU pulse labelling, which labels cells actively undergoing S-Phase, and FACS profiling to exclude differences in the percentage of proliferative cells **(Figure 3 E)**. To investigate the cell cycle length of the NPCs, Hydroxyurea (HU) was used to synchronise the cell-cycle of NPCs at S-G2. Removal of HU then allowed

Downloaded from http://hmg.oxfordjournals.org/ at University of Adelaide on July 3, 2013

NPCs to re-enter the cell cycle, where they were further cultured in the presence of EdU. Cell cycle length was inferred by the number of cells that transitioned through G2, M, G1 and back into S, which is reported by the number of cells labelled by EdU at 0, 8 and 24 hours (41). Surprisingly, we observed a slight but significant reduction (~13%) in the number of NPCs that had transitioned into S-phase at 24 hours, suggesting that loss of Upf3b actually elongated the cell cycle, albeit slightly **(Figure 4 F)**. Having excluded our first two explanations, we reasoned that the increased proliferation might result from increases in the number of initial sphere forming cells in the culture. We applied the well established serial passage sphere-forming assay (42-44). In this assay, a set number of single NPCs are plated at low density following each passage ($1x10^4$ cells / ml; equivalent to conditions used in proliferation assay) and the number of spheres that form in those cultures then counted. Because of the low density conditions, each sphere that forms is derived from a single sphere forming cell, reported to have stem-cell like properties (42-45). These cells typically represent only ~1-5% of the cells derived from neurospheres (39, 42, 45). Cultures lacking Upf3b consistently regenerated more spheres than controls; on average this difference was significant (~1.6 fold greater, 3.7% compared with 5.9%) **(Figure 3 G and Supplementary Figure 14)**. Together this data reveals that loss of Upf3b in NPCs resulted in a growth advantage that is best explained by the expansion of the rare population of sphere-forming cells, that stimulates an increased number of neurospheres that form, and thus the total number of cells in the cultures.

Downloaded from http://hmg.oxfordjournals.org/ at University of Adelaide on July 3, 2013

Loss of Upf3b delays the differentiation of NPCs

As loss of Upf3b promoted the self-renewal of NPCs under conditions that favour the undifferentiated state, we next tested whether these cells would behave similarly under conditions that favour differentiation. We allowed transduced NPCs to adhere to a poly-l-lysine substrate to promote their differentiation into post-mitotic neural cells (39). Following 3 days of adherent culture we analysed the percentage of cells that were still proliferating by pulse labelling with EdU. The loss of Upf3b resulted in a ~1.5 fold increase in the number of cells labelled with EdU **(Figure 4 A and 4 B)**. Next, we reasoned that if differentiation was reduced, colonies derived from single NPCs would have a greater absolute expansive capability (46). We seeded single NPCs at a very low density and allowed them to grow for 6 days (39). The lack of Upf3b resulted in a 35% increase in the number of cells in single NPC derived colonies **(Figure 4 C)**. The increased proliferative and expansive capabilities of NPCs lacking Upf3b were potentially at the expense of differentiated cell types. To test this, we identified the percentages of NPCs and differentiated cell types, namely neurons, astrocytes and oligodendrocytes, in the cultures using immunofluorescent staining of cell type specific marker proteins and cell counts. This labelling regime accounted for greater than 87% of all cells in culture, with similar percentages of unlabelled cells present in both cultures (13% and 7% in control and Upf3b shRNA conditions respectively). At day 3 of differentiation, cultures lacking Upf3b displayed a 52% increase in the percentage of NPCs that was offset by a 41% decrease in the number of differentiated cells **(Figure 4 D and 4 E)**. Next we asked if the loss of Upf3b resulted in loss of a specific neural cell lineage; loss of Upf3b significantly reduced the production of neurons by approximately half, reduced the production of astrocytes (although not statistically significant), whilst

Downloaded from http://hmg.oxfordjournals.org/ at University of Adelaide on July 3, 2013

production of oligodendrocytes was unchanged **(Figure 4 D and 4 E)**. These results indicate that loss of Upf3b-NMD reduced the differentiation of primary E18.5 cortical NPCs.

Upf3b is required for neuronal maturation

The above data demonstrated a role of Upf3b-NMD in regulating mitotic NPC behaviour, but potential high activity of Upf3b-NMD was also recognized in the developing and adult hippocampus, in post-mitotic neuronal populations **(Supplementary Figure 1 and 3 and Figure 2)**. Because this structure is involved in learning and memory, and loss of *UPF3B* function in human results in ID, we decided to investigate the loss of function of *Upf3b* in hippocampal neurons. Primary culture of post-mitotic hippocampal neurons is a well established model of neuronal maturation (37), during which *Upf3b* transcription was elevated **(Figure 2)**. This data suggested that the growth of hippocampal neurons might be sensitive to *Upf3b* function. To address this hypothesis, we again employed lentiviral transduction to deliver the aforementioned control or *Upf3b*-specific shRNAs together with GFP to freshly isolated embryonic hippocampal neurons, and grew them *in-vitro*. By isolating and manipulating post-mitotic neurons, the effects observed in these neurons are independent of any alterations in NPC behaviour. In the following sets of experiments we pooled results from replicate experiments that compared control conditions (WT and S2, n=4 in total) and Upf3b shRNA conditions (T2 and T5, n=4 in total) to again control for both transduction and shRNA off-target effects. At Day 5 of culture, the delivery of *Upf3b* shRNA resulted in an average 83% reduction of *Upf3b* mRNA, which was accompanied by an 81% reduction of protein expression **(Supplementary Figure 15 and Figure 5 A and 5 B).** The loss of Upf3b was accompanied by increased mRNA levels of the three established Upf3b-NMD target reporter genes *Gas5*, *Atf4* and *Snord,* suggesting Upf3b-NMD had indeed been

Downloaded from http://hmg.oxfordjournals.org/ at University of Adelaide on July 3, 2013

disrupted **(Figure 5 C)**. The loss of Upf3b had a small but significant effect on neurite growth **(Figure 5 D-F)**. At day 5 of culture the loss of Upf3b resulted in a 23% reduction in primary axonal length, accompanied by small increases in the arborisation of both axons and dendrites as reported by increases in the number of respective (14-15%) and total (15%) neurite termini. Thus inhibition of Upf3b-NMD was found to regulate the growth of hippocampal neurons in a subtle but specific manner.

Effects of Upf3b loss on alternative NMD and competitive SMD pathway activities

Having discovered alterations in both NPC and neuronal cell behaviours, we next investigated if depletion of Upf3b-NMD led to alternations in alternative NMD and/or competitive SMD pathways. NMD is known to regulate itself in a cell type specific fashion via a negative feedback loop mechanism wherein NMD regulates transcripts encoding NMD factors (40). In both NPCs and hippocampal neurons, the loss of Upf3b-NMD had no effect on the transcript levels of the core NMD factors *Upf1*, *Upf2* or *Upf3a* **(Figure 6 A and 6 B).** Previous work in non-neural cells has established that in the absence of Upf3b, stabilisation of Upf3a protein occurs, and partially compensates for loss of Upf3b function (9, 18). Consistently, western-immunoblot analysis revealed elevated Upf3a levels in both NPCs and hippocampal neurons depleted of Upf3b **(Figure 6 C and 6 D)**. Next we investigated possible alterations of SMD. Intriguingly, whilst *Stau1* appears to have no NMD activating features (data not shown), we observed a 1.5 fold increase in *Stau1* mRNA levels specifically in NPCs (although not obvious by immunoblot analysis), but not in neurons **(Figure 6 A-D)**. Based on this result, and also that SMD efficiency might be improved by default of reduced competitive Upf3b-NMD activities (26, 27), we sought evidence of elevated SMD activity in cells lacking Upf3b. To indicate elevated SMD activity, we investigated the down-regulation

Downloaded from http://hmg.oxfordjournals.org/ at University of Adelaide on July 3, 2013

of the well established SMD targets *cJun*, *Serpine1*, *Gap43* and *Arf1* (28, 29). Whilst in NPCs, *Gap43* expression was significantly down-regulated, the other SMD target transcripts in NPCs, and all SMD target transcripts in hippocampal neurons were not significantly altered by loss of the Upf3b-NMD.

Loss of Upf3b-NMD effects clinically relevant target transcripts in a neural cell specific manner

We recently profiled the transcriptome of lymphoblast cell lines (LCLs) derived from patients harbouring loss-of-function *UPF3B* mutations (9). Of the deregulated genes identified, 16 genes featured that are highly expressed in the brain and display functions related to neural development (9). Because these genes are candidate downstream effectors of UPF3B-NMD that might contribute to the neurological features of the patients, we chose to validate a selection of them using our mouse primary cell populations lacking Upf3b function. We chose 6 genes to validate, 4 of which display conservation of their NMD activating features found in man **(Supplementary Table1).** In NPCs with compromised Upf3b-NMD, 2 of the 6 genes were found to be deregulated; *Six3* expression was increased ~3.6 fold, whilst *Tmod2* expression was decreased ~0.4 fold **(Figure 7)**. In hippocampal neurons with compromised Upf3b-NMD, 2 of the 6 genes were deregulated; *Nrcam* was elevated ~1.4-fold, as was *Robo1* **(Figure 7)**. Thus of the 6 key candidate genes identified using human patient derived LCLs, 4 were also deregulated in mouse neural cells lacking Upf3b-NMD.

Downloaded from http://hmg.oxfordjournals.org/ at University of Adelaide on July 3, 2013

DISCUSSION

Patients with loss of function *UPF3B* mutations present with a highly variable neurological phenotype. This would suggest that *UPF3B* function is important for normal brain development; however, our understanding of the underlying molecular processes is still limited (4-7). In this study we provide a detailed description of *Upf3b* expression and function during brain development in order to gauge into its function. The key findings from our study are: (1) Upf3b expression is developmentally regulated; (2) Loss of Upf3b-NMD promotes the proliferation and reduces differentiation of NPCs and; (3) Loss of Upf3b-NMD affects neurite growth of neurons. Taken together, our data suggest that Upf3b-NMD is a crucial regulator of multiple processes of brain development, which likely underpin aspects of the clinical presentations of variable ID, autism, ADHD and childhood-onset schizophrenia of *UPF3B* patients.

The expression of *Upf3b* suggests complex developmental use of the Upf3b-NMD pathway. *In-situ* hybridisation analysis revealed prominent *Upf3b* expression during embryonic stages of cortical development, as well as in postnatal and adult cortical, hippocampal and cerebellum structures. Focussing on embryonic dorsal forebrain development, our complimentary immunohistological studies revealed a number of phenomena that collectively suggest Upf3b-NMD activity may be regulated by multiple mechanisms that include Upf3b expression and sub-cellular localisation, as well as the activity of the competitive SMD pathway. Firstly, we observed a discontinuity between *Upf3b* mRNA expression and Upf3b protein expression at E14.5 wherein mRNA was strongly expressed in the ventricular zone whilst the protein was not, instead showing high

Downloaded from http://hmg.oxfordjournals.org/ at University of Adelaide on July 3, 2013

expression in the adjacent cortical plate tissue. This implies a level of post-transcriptional control of either *Upf3b* translation or Upf3b stability, the latter of which is observed for the *Upf3b* paralog *Upf3a* (9, 18). This discontinuity was not apparent later at E18.5. Secondly, the nuclear localisation of Upf3b was found to be largely absent in ventricular zone NPC nuclei at E14.5 and earlier, but found present in nuclei of NPCs at later stages and in most cells of neuronal identity. Whilst the significance of this regulation is unclear, it is well established that the function of nuclear-acting factors (e.g. transcription factors) required for embryonic development and cell differentiation can be regulated by the expression of cognate nuclear transport factors (47-49). Such transport factors specific for Upf3b have yet to be identified. Finally, we revealed inverse expression patterns between *Upf3b* and the key component of the SMD pathway *Stau1* in neural cell populations present at E14.5 wherein *Stau1* expression dominated the VZ whereas *Upf3b* expression was dominant in the cortical plate. In line with the molecular control of myogenesis, our data suggests a functional competition between the respective SMD and NMD pathways in NPC and neuronal populations during neurogenesis (26). Consistently, the reduction of Upf3b-NMD in isolated NPCs displayed partial evidence of increased SMD activity. Further demarcation of laminar substructures of the E18.5 cortical wall were also observed when analysed for *Upf3b* and *Stau1* (and *Upf3a*) expression, suggesting continued employment of this mechanism in different cortical neuronal populations. Thus the complex expression of *Upf3b*, and presumably the activity of Upf3b-NMD, appears to be controlled through multiple mechanisms. It is enticing to speculate that the mRNA-protein discontinuity, nuclear localisation and competitive SMD mechanisms might be functionally linked. For example, in cultured cell lines UPF3A is rapidly degraded when access to UPF2 is inhibited (9, 18). Perhaps the exclusion of Upf3b from nuclear regions, and thus presumably Upf2,

Downloaded from http://hmg.oxfordjournals.org/ at University of Adelaide on July 3, 2013

results in a similar destabilisation that might explain the overall reduced protein expression in the ventricular zone NPCs at E14.5 and earlier, and dominance of Stau1 expression. Consistently, Upf3b expression was much higher in populations displaying prominent nuclear localisation, namely neurons in the cortical plate at E14.5, and ventricular zone and cortical plate cells at E18.5. Finally differences in the expression of Upf3b, Upf3a and Stau1 within post-mitotic neurons also suggested that these factors may harbour divergent functions (i.e. outside of NMD and SMD), or that their represented NMD and SMD pathways may are compartmentalised in some way. Certainly for Stau1, functions in mRNA transport are well established in neuronal cells (50), whilst previous descriptions of Upf3b localisation to synapse structures have also suggested functions outside of NMD (5).

NPCs populating the ventricular zone at E18.5 and hippocampal neurons were identified as cell types in which Upf3b-NMD is likely to be highly active based on: (1) high mRNA and protein expression; (2) nuclear localisation and; (3) comparable or dominant expression over *Stau1* and *Upf3a*. We thus reasoned these cells might be sensitive to loss of Upf3b-NMD activity, and that such manipulation might reveal pathological mechanisms that in-part explain the clinical phenotype in patients with *UPF3B* mutations. Indeed, loss of Upf3b-NMD in both of these cell types affected their behaviour. In NPCs, grown as neurospheres, loss of Upf3b-NMD promoted the expansion of sphere-forming cells, which are known to display the bona-fide neural stem cell properties of long-term self-renewal and multipotency (42, 45, 51). Interestingly, the cell cycle length of neurosphere cells was actually slightly increased, which perhaps also reflects a higher percentage of neural stem-like cells, which do display longer cell cycling times than ‘transient amplifying’ progenitor cells (52). When these cells were grown under conditions that favour their differentiation,

Downloaded from http://hmg.oxfordjournals.org/ at University of Adelaide on July 3, 2013

the loss of Upf3b-NMD promoted expansion of NPCs, at the expense of producing differentiated cells. Together, these phenomena are consistent with our expression studies which correlated progressively increased *Upf3b* expression (i.e. from ventricular zone NPCs at E10.5 to E18.5, and to post-mitotic neurons), and thus likely Upf3b-NMD activity, with less inherent proliferative and expansive behaviours (52). Intriguingly, previously reported loss of Upf1 in NPCs has an opposing effect wherein differentiation was promoted (53). This suggests involvement of Upf1 in pathways outside of Upf3b-NMD, which is well established, and includes for example SMD (28, 29). Consistent with this, both Upf1 and Stau1 were highly expressed in the VZ at earlier stages of forebrain development (e.g. E10.5 – E14.5) when Upf3b expression was low, suggesting predominance of this alternative pathway. It is thus likely that loss of both SMD and NMD, and additional functions of Upf1 outside of mRNA decay (10), are driving the overriding differentiation processes in response to loss of Upf1.

Our current findings also add to the established roles of the NMD factors Upf3b and Upf2 in differentiation processes (26). In the myogenic differentiation of C1C12 cells, Upf2-dependent NMD promoted the undifferentiated state via direct NMD of *Myogenin*, which encodes a master regulator of differentiation, whilst Upf3b-NMD correlated with, and SMD activity promoted differentiation, via SMD of *Pax3*, which encodes a master regulator of the myoblasts (26). Our data likewise implicates Upf3b-NMD in the promotion of neural differentiation, and suggests *Six3*, a master regulator of cortical and visual development in mouse and man, as a direct target (54-56). *Six3* mRNA contains an uORF NMD feature and has been identified as an NMD target also in *UPF3B* patient LCLs (9). As with loss of Upf3b, over-expression of *Six3* in mouse cortical NPCs results in their expansion and reduction in

Downloaded from http://hmg.oxfordjournals.org/ at University of Adelaide on July 3, 2013

differentiation, suggesting it might link the loss of Upf3b-NMD to the observed expansion and reduced differentiation of NPCs (46). Also consistent with the functional balance between NMD and SMD pathways in controlling differentiation processes, loss of Upf3b also resulted in modest increases in Stau1 mRNA expression and partial evidence of increased SMD activity in NPCs. More rigorous investigations into this regulatory mechanism in neural differentiation will need loss of Upf2 approaches, or compound Upf3b-Upf3a loss, as the loss of Upf3b alone was compensated by increased Upf3a stabilisation, which suggests partial maintenance of the NMD-SMD balance.

We also extended our loss of function approach to study post mitotic neuronal growth in hippocampal neurons. Because these cells were isolated and manipulated as a pure population of post-mitotic neurons (37), the effects observed from the loss of Upf3b are independent of the earlier NPC defects. We revealed that loss of Upf3b-NMD in hippocampal neurons results in a reduction in axonal length associated with subtle increases in neurite arborisation. Consistent with the involvement of NMD in neurite growth, previous reports have established that down regulation of *Upf1* is associated with increased dendritic spine length (53). We observed progressive increases in the transcription of *Upf3b* during neuronal growth *in-vitro*, which was also suppressed by chronic depolarisation in mature cells. Together, these data suggest that neuronal growth and functions are sensitive to Upf3b function. Indeed we have previously postulated neurite growth defects as a pathological feature in *UPF3B* patients; in patient cells, compromised NMD results in direct upregulation of *ARHGAP24*, which when overexpressed in mouse hippocampal neurons, results in reduction of axonal length and neurite arborisation (9). Unlike in humans however, mouse *Arhgap24* does not have the NMD targeting uORF feature and is not

Downloaded from http://hmg.oxfordjournals.org/ at University of Adelaide on July 3, 2013

upregulated in response to loss of Upf3b-NMD (data not shown). Despite this, loss of Upf3b-NMD still led to altered neuronal growth.

Using our candidate gene approach, we identified upregulation of *Robo1* and *Nrcam* as putative Upf3b-NMD targets in mouse hippocampal neurons, which consistently participate in axon guidance and axon growth (57-60). Furthermore, both the *Robo* pathway and *Nrcam* gene have been previously identified in cells deficient in *Upf1* as NMD targets (53). Others have identified the *ARC*, *PSD95* and *PTBP2* transcripts, which encode proteins harbouring vital neural functions, as being critically regulated by NMD (33-36), although this set of genes was not supported by studies of *UPF3B* patient LCLs (9). Thus it is likely that cell-type specific batteries of Upf3b-NMD regulated genes are responsible for the coordination of NPC differentiation and subsequent neuronal growth and function. Indeed, UPF3B-NMD is known to result in deregulation of ~5% of the transcriptome (9).

In humans, loss of function mutations in *UPF3B* result in ID accompanied by a spectrum of additional neurological features that may include autism, attention deficit hyperactivity disorder, childhood-onset schizophrenia or dysmorphic features including macrocephaly and visual impairment (4-7). In this study, we aimed to model this disorder at a neural cell level by disabling Upf3b-NMD in highly physiologically relevant cells. The alterations in cellular and molecular mechanisms we have identified using these models are consistent with patient's clinical presentations. Specifically, our data suggest that the neuronal networks of the hippocampus might be affected, which we can plausibly speculate to cause or at least contribute to patients' ID. That *Nrcam* and *Robo1* mRNA expression is deregulated in these cells and also in human patients, brings this high-ranking molecular mechanisms into the broader picture (9). *Nrcam* is an autism susceptibility gene and null

Downloaded from http://hmg.oxfordjournals.org/ at University of Adelaide on July 3, 2013

mice display autistic behaviours reminiscent of clinical features of *UPF3B* patients (61-64). Likewise, the expansion of NPCs in our assays could explain the macrocephalic features in some *UPF3B* patients. The common deregulation of *Six3* in both NPCs and in *UPF3B* patients provides a high-ranking candidate molecular mechanism for the macrocephaly, and might also account for the visual impairment of some *UPF3B* patients (46, 54-56).

The spectrum of phenotypes seen in *UPF3B* patients, which also shows intra-familial variability, presents a challenge to identify disease modifying factors (9). Whilst varying UPF3A protein stability appears to be one of the candidate modifying factors, other genes and proteins might also be contributing (9). Our study of loss of *Upf3b* function has identified additional candidates to be investigated, revealing both cellular and molecular mechanisms contributing to the pathology and thus clinical outcomes of *UPF3B* patients.

MATERIALS AND METHODS.

Animal Use

This study was performed under regulations of the South Australian Animal Welfare Act 1986, and in strict accordance with the Australian Code of Practice for the Care of Animals for Scientific Purposes, 2004. The protocol was approved by the Women's and Children's Health Network (WCHN) Animal Ethics Committee (Approval Number: 750/06/2011 and 888/06/13). All euthanasia was performed using cervical dislocation, and every effort was made to minimize suffering. Time-mated pregnant female Swiss mice were obtained from the Women's and Children's Health Network Animal Care Facility (Women's and Children's Hospital, Adelaide, Australia).

Downloaded from http://hmg.oxfordjournals.org/ at University of Adelaide on July 3, 2013

Immunohistochemistry

Tissue was fixed using phosphate buffered saline (PBS) containing 4% paraformaldehyde (4%PFA-PBS). Tissue was processed and stained as previously described (65). Antigen retrieval was performed by imersing sections for 20 minutes in a heated solution of 0.01M sodium citrate, pH=6 or Tris-EDTA pH=9. Primary and secondary antibodies were used at the following dilutions; sheep anti-UPF3b (1:200; in-house, (4)), rabbit anti-UPF3B (1:50), mouse anti-UPF3A (1:100) and rabbit anti-βIII tubulin (1:200; all from Sigma), rabbit anti-STAU1 (1:100; Chemicon, Millipore Bioscience Research Products, Billerica, MA), donkey anti-sheep Alexafluor555, donkey anti-rabbit Alexafluor488 and donkey anti-mouse Alexafluor647 (all 1:800; Invitrogen, Carlsbad, CA). Non-specific staining was controlled by using secondary-only controls (data not shown)

In-situ Hybridisation

In-situ probes were cloned into pGEM-T vectors using TA cloning technique as per manufactures instructions (Promega, Madison, WI). PCR amplification of probes from cDNA was achieved using Taq Polymerase (Roche, Penzberg, Germany) and the primer pairs listed in **Supplementary Table 2**. Probe containing pGemT vectors were linearised and in-vitro transcribed in both sense and anti-sense direction using the DIG RNA Labelling Kit as per manufactures instructions (Roche). DNAse treated RNA probes were purified using Chromaspin100 colomns (GE Health care, Uppsala, Sweden), and quantified. Parrafin sections were rehydrated, and treated with 4%PFA-PBS for 20mins. Sections were then ProteinaseK treated (20ug/ml in PBS) for 8 minutes at 37°C, followed by another 5min

Downloaded from http://hmg.oxfordjournals.org/ at University of Adelaide on July 3, 2013

treatment with 4%PFA-PBS. Sections were acetylated for 10minutes using a solution of 0.1M triethanolamine containing 0.25% (v/v) acetic anhydride (both from Sigma Aldridge, St Louis, MO). After washing with PBS, sections were dehydrated using an ethanol series, and allowed to air dry for same-day probing. 300ng of either sense or anti-sense was added to 200µl of hybridisation mix (50% formamide (v/v), 0.3M NaCl, 20mM Tris-HCL, 5mM EDTA, 10% Dextran sulphate (w/v), 1x Denhardts, 0.005% tRNA (w/v); all from Sigma Aldridge) and added to slides. Slides were incubated at 65°C O/N in a chamber humidified with a solution of 50% formamide, 1xSSC. Following hybridisation, sections were washed 3 times in 2xSSC, twice in 50% formamide-2%SSC, twice in 2xSSC, twice in 0.2%SSC all for 20mins at 65°C. For DIG detection, Sections were blocked in an incubation solution (0.1M Tris pH7.6, 0.15M NaCl) supplemented with 10% inactivated sheep serum (v/v; ISS). Sheep Anti-DIG antibody was diluted 1:1000 into incubation solution containing 3% ISS and added to sections O/N at 4°C. Sections were washed 3x with incubation solution, and twice with detection solution (0.1M Tris-HCl pH9.5, 0.1M NaCl and 0.05M MgCl). NBT and BCIP (Roche) were added to detection solution containing 5% PVA (Sigma) and added to slides and incubated at RT in the dark. Following development of signal, sections were extensively washed in water before being dehydrated through an ethanol series and allowed to air dry before mounting in Vector Mount.

Generation of Lentivirus

Tet-inducible and constitutive 3rd generation lentiviral vectors were employed as previously described (66, 67). To generate Upf3b specific shRNA transfer vectors, 6 shRNA sequences predicted to target Upf3b were designed using BLOCK-it RNAi designer software

Downloaded from http://hmg.oxfordjournals.org/ at University of Adelaide on July 3, 2013

(Invitrogen). The shRNA sequences can be found in **Supplementary Table 3**. Two control shRNA sequences were used, including a scrambled T2 trigger called S2 and a shRNA targeted to luciferase called Luc. Sequences can be found in **Supplementary Table 3**. These sequences were used in the triple-step PCR protocol to generate the sense-loop-antisense structure flanked 5' by a *att*B1 recombination site and a TH1 promoter, and 3' by a termination signal and *att*B2 recombination site as previously described (66). Gateway based BP reactions (Invitrogen) shuttled these shRNA sequences into pDONR207, and subsequently LR reactions (Invitrogen) shuttled the sequences into either the tet-regulatable destination lentiviral transfer vector plv-T-shRNA (66), or a re-engineered constitutively expressing version lacking the tet regulatory protein (T-Rex)-ires casette, which we called plv-C-shRNA.

To generate lentiviral stocks, ~$1x10^7$ Hek293 cells in a T75 flask were transfected O/N with 12.5 µg of transfer vector (plv-t-sh or plv-C-sh), 7.5 µg of Gag/Pol (D8.2), 6.25 mg of Rev (pRSV-Rev), and 3.75 µg of Env (pCMV-VSV-G), using Lipofectamine 2000 reagent as per manufactures instructions (Invitrogen). Medium was replaced with 10 ml of fresh DMEM and left for 48hrs. Supernatant was collected, filtered (pore size, 0.45 mm), and concentrated 200x by ultracentrifugation at 20,000 rpm for 90 min. Virus titre was determined using a limiting dilution, as described previously (67).

Transduction of neurons was performed at either MOI=1 for single cell mophometric analysis, or MOI=30 for biochemical analysis O/N at day 1 of culture. Transduction of NPCs was achieved at MOI=10 using O/N incubation with dissociated cells derived from secondary neurospheres. Following sphere re-formation, cells were dissociated and GFP+ve cells were purified using Fluorescent Activated Cell Sorting (FACS; BD FACSAriaII flow cytometer; BD

Downloaded from http://hmg.oxfordjournals.org/ at University of Adelaide on July 3, 2013

Bioscience, San Jose, CA), for further culture as neurospheres. Cells remain >95% GFP positive after 7 passages (data not shown).

Cell culture

Feeder independent R1 Embryonic stem cells (ESCs) were cultured and differentiated as described previously (65). Isolation of neural progenitor cells (NPCs) from the E18 cortex was as previously described (68). Single cells for NPC assays were generated by passing dissociated cells through a 0.75µm cell filter (BD Biosciences). All neural progenitor cell assays were conducted in biological triplicate, with each replicate representing a separate clonal cell line derived from the transduction of a different lentiviral shRNA particle (or combination of particles). Averages of these triplicate results are reported. The cell proliferation assay was conducted using the Cell Titre 96AQueous Kit (Promega) as per manufactures instruction; each biological replicate was analysed using technical quadruplicates and normalised against starting cell numbers (10^3±4.2% cells per well). Cell cycle analysis was conducted as previously described (41). Briefly, cells were synchronised using a 22 hour incubation in 2mM Hydroxyurea (HU; Sigma). Cells were washed 4 times in fresh NPC media to remove traces of HU before further culture in NPC media containing 10µM 5-ethynyl-2'-deoxyuridine (EdU; Invitrogen). EdU pulse assays were performed as previously described (69). Neurosphere cultures were labelled for 4 hours at 3 days post passaging. Adherent cultures were labelled for 8 hours at day 3 of culture. EdU incorporation was labelled using the Click-it EdU AlexaFluor647-Azide Flow Cytometry Kit as per manufactures instructions (Invitrogen). EdU was detected within Enhanced Green Fluorescent Protein (EGFP) expressing cells using either FACS profiling of dissociated

Downloaded from http://hmg.oxfordjournals.org/ at University of Adelaide on July 3, 2013

neurosphere cells or by immunofluorescent microscopy and cell counts (see below). For FACS analysis, the biological triplicate experiments were analysed using technical triplicates. Sphere forming assays were performed by culturing cells at a low, clonal density ($1x10^4$ cells/ml). Colony forming and differentiation assays were performed by plating dissociated cells onto poly-l-lysine (Sigma) coated coverslips (Menzel-glasser, Thermo Fisher Scientific, Waltham, MA) at $1x10^3$ cells/cm^2 or $1x10^4$/cm^2 respectively, and culturing cells in Neuropshere media with or without EGF. For colony formation, cells were cultured for 6 days without EGF before fixation. For differentiation, cells were cultured for 3 days with EGF and then fixed. Immunofluorescent staining and Fluorescent Microscopy (see below) was used for cell count analysis. For the colony size assay, at least 100 colonies were scored in each replicate (total n=360 control, and n=546 $Upf3b^{shRNA}$). For analysis of differentiation, at least 300 cells were scored for each replicate experiment (progenitor cells: total n=1609 control, and n=1486 $Upf3b^{shRNA}$; neurons: total n=1868 control, and n=1208 $Upf3b^{shRNA}$; astrocytes: total n=2898 control, and n=2244 $Upf3b^{shRNA}$; oligodendrocytes: total n=2233 control, and n=1203 $Upf3b^{shRNA}$; EdU incorporation: n=1063 control; n=1234 $Upf3b^{shRNA}$. Isolation of primary hippocampal and cortical neurons was as described previously (69). Biochemical assays were done in quadruplicate (2 biological replicates each representing transduction with separate lentiviral control or Upf3b shRNA particles). All data represents average of 2 biological experiments conducted twice (total n=4 control, and n=4 $Upf3b^{shRNA}$). Morphometric assays were done using biological triplicate, with each replicate representing transduction with either S2 or T2 shRNA lentiviral particles (see above). Analysis was conducted using Immunofluorescent staining and Fluorescent Microscopy (see below). For each replicate, at least 30 neurons were scored (total n=98 control n=99) using the ImageJ software package (NIH).

Downloaded from http://hmg.oxfordjournals.org/ at University of Adelaide on July 3, 2013

Immunoflourescence

Cultured cells were fixed with 4%PFA-PBS for 15 minutes at R/T. Cells were block-permeablised using PBST-10%NDS for 1 hour at R/T. Primary and secondary antibodies were incubated in PBST-3%NDS overnight (O/N) at 4°C and 1h at RT respectively at the following dilutions; chicken anti-MAP2, mouse anti-CNPAse, mouse anti-Tau1 (all at 1:2000; Chemicon), rabbit anti-GFAP, goat anti-GFAP, mouse anti-βIII-tubulin, rabbit anti-βIII-tubulin (all at 1:300; Sigma-Aldridge), rabbit anti-Pax6 (1:200; Chemicon), sheep anti-Upf3b (1:200, in house), donkey anti-sheep Alexafluor555, donkey anti-rabbit Alexafluor488/555/647 and donkey anti-mouse Alexafluor488/555/647 (all 1:1000; Invitrogen), donkey anti-chickenCy3 (Jackson Laboartories, Bar Harbour , ME). Cells were counterstained with DAPI and mounted with Slow-fade mounting media (both from Invitrogen). Non-specific staining was controlled by using secondary-only controls (data not shown).

Microscopy

Fluorescence was viewed using the Axioplan2 microscope (Carl Zeiss, Jena, Germany) fitted with an HBO 100 lamp (Carl Zeiss). Images were captured using an Axiocam Mrm camera and Axio Vs40 v4.5.0.0 software (Axiovision, Carl Zeiss). To produce optical sections of brain samples, images were produced using this system fitted with the ApoTome slider module (Carl Zeiss). Quantification of fluorescent staining of brain sections was conducted as previously described with modifications (70). Exposure times during image capture were kept constant at 100μs, to maintain reproducibility. Use of neutral density filters was

Downloaded from http://hmg.oxfordjournals.org/ at University of Adelaide on July 3, 2013

employed (and kept constant) to ensure all signals were captured within the linear response range. Following image capture, tissue areas (e.g. ventricular zones, cortical plates, or entire radial cortical wall sections) were selected as a region of interest (ROI) using ImageJ software. Average pixel intensities per unit area, or plot profiles of pixel intensities were generated using ImageJ analysis suite. Background pixel intensity was derived from "secondary antibody only" negative control stains. Average Upf3b pixel intensities across developmental stages was background subtracted and normalised using average DAPI pixel intensity as a control. Range in average pixel intensity of DAPI stains was ±6.5%. Experiments (including negative controls) were conducted on at least 6 brains at each developmental stage. Results represent the average of each experiment, error bars represent standard deviation. Upf3b pixel intensity profiles within ROIs were normalised against cell density using the associated DAPI pixel intensity profile. Colorimetric sections were observed with an Olympus BH-2 microscope (Olympus, Tokyo, Japan) or an Olympus SZX16 dissecting microscope (Olympus) and images captured using a SPOT-insight colour camera v3.2.0 (Diagnostic Instruments USA, Sterling Heights, MI) with Image Pro-Plus v5.1.2.59 software (Media Cybernetics Inc., Bethesda, MD).

Downloaded from http://hmg.oxfordjournals.org/ at University of Adelaide on July 3, 2013

Biochemical Analysis

Protein was isolated from cells using a lysis buffer (120 mM NaCl, 50 mM Tris-HCl (pH 8.0), 0.5% NP-40 (v/v), 1× protease inhibitor cocktail (Sigma), 1 mM Na3VO4, 1 mM NaF, 1 mM PMSF) and quantitated using Bradford assay (Biorad, Hercules, CA). Samples were separated and transferred to nitrocellulose (Biotrace NT, Pall Corporation, New York, NY) using the NuPage precast gel system as per manufactures instructions (Invitrogen). Blots were

blocked using PBST containing 5%NHS and 5% skim milk. Antibodies were incubated in this same solution at the following dilutions; sheep anti-Upf3b (1:10000; in house), mouse anti-β-actin (1:5000; Sigma-Aldridge), rabbit-anti Stau1 (1:300; Chemicon), mouse anti-Upf3a (1:300; Sigma), mouse anti-goat/sheep-HRP, goat anti-rabbit-HRP and goat anti-mouse HRP (all 1:1000; Dako, Glostrup, Denmark). RNA was isolated from cells/tissues using Trizol reagent as per manufactures instructions (Invitrogen) and further processed using the RNAeasy kit including DNAse treatment (Qiagen, Germantown, MD). cDNA was generated using SuperscriptIII reverse transcriptase as per manufactures instructions (Invitrogen) using random hexamer priming (Geneworks, Adelaide, Australia). The StepOne platform and software (Applied Biosciences, Invitrogen) was employed for qPCR analysis. PCR reactions were generated using the sybr green master mix as per manufactures instructions (Biorad) and run using the following parameters; 95°C – 5 minutes; 35 cycles of: 95°C - 10sec, 60°C – 30sec; followed a melt curve increment step 60°C-100°C. All primers used met strict quality control parameters amplifying control cDNA at 100±10% efficiencies, and producing only single PCR products. Primers for β-actin, BLBP, Sox1, Oct4 and βIII-tubulin are as previously described (Jolly et al 2009), for Atf4, Gas5 and Snord as previously described (Huang et al 2007), and for others as listed in **Supplementary Table 4.**

Downloaded from http://hmg.oxfordjournals.org/ at University of Adelaide on July 3, 2013

ACKNOWLEDGEMENTS

We thank David Bersten, University of Adelaide, Adelaide, Australia, for providing the ply-C-shRNA plasmid, Anand Srivastava and Charles Schwartz, Greenwood Genetic Centre, Greenwood, USA, for providing the Upf3b hypomorphic ES cell line, and Silvia Nobbs, Women's and Children's Health Network, Adelaide, Australia, and Dr. Randall Gross, Women's and Children's Health Institute, Adelaide, Australia, for technical assistance with FACS. This work was supported by the Australian NH&MRC [Project Grant 453457 to JG] and the Women's and Children's Hospital Foundation [Grant to LJ]. JG is supported by NH&MRC Principal Research Fellowship.

CONFLICT OF INTEREST STATEMENT

The authors declare no conflicts of interest.

Downloaded from http://hmg.oxfordjournals.org/ at University of Adelaide on July 3, 2013

REFERENCES

1 Ropers, H.H. (2010) Genetics of early onset cognitive impairment. *Annu. Rev. Genomics. Hum. Genet.,* **11**, 161-187.

2 Doran, C.M., Einfeld, S.L., Madden, R.H., Otim, M., Horstead, S.K., Ellis, L.A. and Emerson, E. (2012) How much does intellectual disability really cost? First estimates for Australia. J *Intellect. Dev. Disabil.*, **37**, 42-49.

3 Gecz, J., Shoubridge, C. and Corbett, M. (2009) The genetic landscape of intellectual disability arising from chromosome X. *Trends Genet.*, **25**, 308-316.

4 Tarpey, P.S., Raymond, F.L., Nguyen, L.S., Rodriguez, J., Hackett, A., Vandeleur, L., Smith, R., Shoubridge, C., Edkins, S., Stevens, C. et al. (2007) Mutations in UPF3B, a member of the nonsense-mediated mRNA decay complex, cause syndromic and nonsyndromic mental retardation. *Nat. Genet*., **39**, 1127-1133.

5 Laumonnier, F., Shoubridge, C., Antar, C., Nguyen, L.S., Van Esch, H., Kleefstra, T., Briault, S., Fryns, J.P., Hamel, B., Chelly, J. et al. (2010) Mutations of the UPF3B gene, which encodes a protein widely expressed in neurons, are associated with nonspecific mental retardation with or without autism. *Mol. Psychiatry*, **15**, 767-776.

6 Lynch, S.A., Nguyen, L.S., Ng, L.Y., Waldron, M., McDonald, D. and Gecz, J. (2012) Broadening the phenotype associated with mutations in UPF3B: Two further cases with renal dysplasia and variable developmental delay. *Eur. J. Med. Genet*., **55**, 476-479.

7 Addington, A.M., Gauthier, J., Piton, A., Hamdan, F.F., Raymond, A., Gogtay, N., Miller, R., Tossell, J., Bakalar, J., Inoff-Germain, G. et al. (2011) A novel frameshift mutation in UPF3B identified in brothers affected with childhood onset schizophrenia and autism spectrum disorders. *Mol. Psychiatry*, **16**, 238-239.

Downloaded from http://hmg.oxfordjournals.org/ at University of Adelaide on July 3, 2013

8 Xu, X., Zhang, L., Tong, P., Xun, G., Su, W., Xiong, Z., Zhu, T., Zheng, Y., Luo, S., Pan, Y. et al. (2012) Exome sequencing identifies UPF3B as the causative gene for a Chinese non-syndrome mental retardation pedigree. *Clin. Genet*. **83**, 560-564.

9 Nguyen, L.S., Jolly, L., Shoubridge, C., Chan, W.K., Huang, L., Laumonnier, F., Raynaud, M., Hackett, A., Field, M., Rodriguez, J. et al. (2011) Transcriptome profiling of UPF3B/NMD-deficient lymphoblastoid cells from patients with various forms of intellectual disability. *Mol. Psychiatry*, **17**, 1103-1115.

10 Nicholson, P., Yepiskoposyan, H., Metze, S., Zamudio Orozco, R., Kleinschmidt, N. and Muhlemann, O. (2010) Nonsense-mediated mRNA decay in human cells: mechanistic insights, functions beyond quality control and the double-life of NMD factors. *Cell. Mol. Life Sci*., **67**, 677-700.

11 Gehring, N.H., Neu-Yilik, G., Schell, T., Hentze, M.W. and Kulozik, A.E. (2003) Y14 and hUpf3b form an NMD-activating complex. *Mol. Cell*., **11**, 939-949.

12 Kim, V.N., Kataoka, N. and Dreyfuss, G. (2001) Role of the nonsense-mediated decay factor hUpf3 in the splicing-dependent exon-exon junction complex. *Science*, **293**, 1832-1836.

13 Chamieh, H., Ballut, L., Bonneau, F. and Le Hir, H. (2008) NMD factors UPF2 and UPF3 bridge UPF1 to the exon junction complex and stimulate its RNA helicase activity. *Nat. Struct. Mol. Biol*., **15**, 85-93.

14 Kashima, I., Yamashita, A., Izumi, N., Kataoka, N., Morishita, R., Hoshino, S., Ohno, M., Dreyfuss, G. and Ohno, S. (2006) Binding of a novel SMG-1-Upf1-eRF1-eRF3 complex (SURF) to the exon junction complex triggers Upf1 phosphorylation and nonsense-mediated mRNA decay. *Genes Dev*., **20**, 355-367.

15 Ivanov, P.V., Gehring, N.H., Kunz, J.B., Hentze, M.W. and Kulozik, A.E. (2008) Interactions between UPF1, eRFs, PABP and the exon junction complex suggest an integrated model for mammalian NMD pathways. *EMBO J*., **27**, 736-747.

Downloaded from http://hmg.oxfordjournals.org/ at University of Adelaide on July 3, 2013

16 Singh, G., Rebbapragada, I. and Lykke-Andersen, J. (2008) A competition between stimulators and antagonists of Upf complex recruitment governs human nonsense-mediated mRNA decay. *PLoS Biol*., **6**, e111.

17 Chan, W.K., Huang, L., Gudikote, J.P., Chang, Y.F., Imam, J.S., MacLean, J.A., 2nd and Wilkinson, M.F. (2007) An alternative branch of the nonsense-mediated decay pathway. *EMBO J*., **26**, 1820-1830.

18 Chan, W.K., Bhalla, A.D., Le Hir, H., Nguyen, L.S., Huang, L., Gecz, J. and Wilkinson, M.F. (2009) A UPF3-mediated regulatory switch that maintains RNA surveillance. *Nat. Struct. Mol. Biol*., **16**, 747-753.

19 Mendell, J.T., Sharifi, N.A., Meyers, J.L., Martinez-Murillo, F. and Dietz, H.C. (2004) Nonsense surveillance regulates expression of diverse classes of mammalian transcripts and mutes genomic noise. *Nat. Genet*., **36**, 1073-1078.

20 Wittmann, J., Hol, E.M. and Jack, H.M. (2006) hUPF2 silencing identifies physiologic substrates of mammalian nonsense-mediated mRNA decay. *Mol. Cell. Biol*., **26**, 1272-1287.

21 Weischenfeldt, J., Damgaard, I., Bryder, D., Theilgaard-Monch, K., Thoren, L.A., Nielsen, F.C., Jacobsen, S.E., Nerlov, C. and Porse, B.T. (2008) NMD is essential for hematopoietic stem and progenitor cells and for eliminating by-products of programmed DNA rearrangements. *Genes Dev*., **22**, 1381-1396.

22 Rehwinkel, J., Letunic, I., Raes, J., Bork, P. and Izaurralde, E. (2005) Nonsense-mediated mRNA decay factors act in concert to regulate common mRNA targets. RNA, **11**, 1530-1544.

23 He, F., Li, X., Spatrick, P., Casillo, R., Dong, S. and Jacobson, A. (2003) Genome-wide analysis of mRNAs regulated by the nonsense-mediated and 5' to 3' mRNA decay pathways in yeast. *Mol. Cell*, **12**, 1439-1452.

Downloaded from http://hmg.oxfordjournals.org/ at University of Adelaide on July 3, 2013

24 Medghalchi, S.M., Frischmeyer, P.A., Mendell, J.T., Kelly, A.G., Lawler, A.M. and Dietz, H.C. (2001) Rent1, a trans-effector of nonsense-mediated mRNA decay, is essential for mammalian embryonic viability. *Hum. Mol. Genet*., **10**, 99-105.

25 Gehring, N.H., Kunz, J.B., Neu-Yilik, G., Breit, S., Viegas, M.H., Hentze, M.W. and Kulozik, A.E. (2005) Exon-junction complex components specify distinct routes of nonsense-mediated mRNA decay with differential cofactor requirements. *Mol. Cell*., **20**, 65-75.

26 Gong, C., Kim, Y.K., Woeller, C.F., Tang, Y. and Maquat, L.E. (2009) SMD and NMD are competitive pathways that contribute to myogenesis: effects on PAX3 and myogenin mRNAs. *Genes Dev*., **23**, 54-66.

27 Maquat, L.E. and Gong, C. (2009) Gene expression networks: competing mRNA decay pathways in mammalian cells. *Biochem. Soc. Trans*., **37**, 1287-1292.

28 Kim, Y.K., Furic, L., Desgroseillers, L. and Maquat, L.E. (2005) Mammalian Staufen1 recruits Upf1 to specific mRNA 3'UTRs so as to elicit mRNA decay. *Cell*, **120**, 195-208.

29 Kim, Y.K., Furic, L., Parisien, M., Major, F., DesGroseillers, L. and Maquat, L.E. (2007) Staufen1 regulates diverse classes of mammalian transcripts. *EMBO J*., **26**, 2670-2681.

30 Silver, D.L., Watkins-Chow, D.E., Schreck, K.C., Pierfelice, T.J., Larson, D.M., Burnetti, A.J., Liaw, H.J., Myung, K., Walsh, C.A., Gaiano, N. et al. (2010) The exon junction complex component Magoh controls brain size by regulating neural stem cell division. *Nat. Neurosci*., **13**, 551-558.

31 Wittkopp, N., Huntzinger, E., Weiler, C., Sauliere, J., Schmidt, S., Sonawane, M. and Izaurralde, E. (2009) Nonsense-mediated mRNA decay effectors are essential for zebrafish embryonic development and survival. *Mol. Cell. Biol*., **29**, 3517-3528.

32 Long, A.A., Mahapatra, C.T., Woodruff, E.A., 3rd, Rohrbough, J., Leung, H.T., Shino, S., An, L., Doerge, R.W., Metzstein, M.M., Pak, W.L. et al. (2010) The nonsense-mediated decay

Downloaded from http://hmg.oxfordjournals.org/ at University of Adelaide on July 3, 2013

pathway maintains synapse architecture and synaptic vesicle cycle efficacy. *J. Cell Sci*., **123**, 3303-3315.

33 Boutz, P.L., Stoilov, P., Li, Q., Lin, C.H., Chawla, G., Ostrow, K., Shiue, L., Ares, M., Jr. and Black, D.L. (2007) A post-transcriptional regulatory switch in polypyrimidine tract-binding proteins reprograms alternative splicing in developing neurons. *Genes Dev*., **21**, 1636-1652.

34 Makeyev, E.V., Zhang, J., Carrasco, M.A. and Maniatis, T. (2007) The MicroRNA miR-124 promotes neuronal differentiation by triggering brain-specific alternative pre-mRNA splicing. *Mol. Cell*, **27**, 435-448.

35 Zheng, S., Gray, E.E., Chawla, G., Porse, B.T., O'Dell, T.J. and Black, D.L. (2012) PSD-95 is post-transcriptionally repressed during early neural development by PTBP1 and PTBP2. *Nat. Neurosci*., **15**, 381-388, S381.

36 Giorgi, C., Yeo, G.W., Stone, M.E., Katz, D.B., Burge, C., Turrigiano, G. and Moore, M.J. (2007) The EJC factor eIF4AIII modulates synaptic strength and neuronal protein expression. *Cell*, **130**, 179-191.

37 Kaech, S. and Banker, G. (2006) Culturing hippocampal neurons. *Nat. Protoc*., **1**, 2406-2415.

38 Murase, S., Mosser, E. and Schuman, E.M. (2002) Depolarization drives beta-Catenin into neuronal spines promoting changes in synaptic structure and function. *Neuron*, **35**, 91-105.

39 Giachino, C., Basak, O. and Taylor, V. (2009) Isolation and manipulation of mammalian neural stem cells in vitro. *Methods Mol. Biol*., **482**, 143-158.

40 Huang, L., Lou, C.H., Chan, W., Shum, E.Y., Shao, A., Stone, E., Karam, R., Song, H.W. and Wilkinson, M.F. (2011) RNA homeostasis governed by cell type-specific and branched feedback loops acting on NMD. *Mol. Cell*, **43**, 950-961.

Downloaded from http://hmg.oxfordjournals.org/ at University of Adelaide on July 3, 2013

41 Kouroupi, G., Lavdas, A.A., Gaitanou, M., Thomaidou, D., Stylianopoulou, F. and Matsas, R. (2010) Lentivirus-mediated expression of insulin-like growth factor-I promotes neural stem/precursor cell proliferation and enhances their potential to generate neurons. *J. Neurochem.*, **115**, 460-474.

42 Rietze, R.L., Valcanis, H., Brooker, G.F., Thomas, T., Voss, A.K. and Bartlett, P.F. (2001) Purification of a pluripotent neural stem cell from the adult mouse brain. *Nature*, **412**, 736-739.

43 Capela, A. and Temple, S. (2002) LeX/ssea-1 is expressed by adult mouse CNS stem cells, identifying them as nonependymal. *Neuron*, **35**, 865-875.

44 Kim, M. and Morshead, C.M. (2003) Distinct populations of forebrain neural stem and progenitor cells can be isolated using side-population analysis. *J. Neurosci.*, **23**, 10703-10709.

45 Reynolds, B.A. and Weiss, S. (1996) Clonal and population analyses demonstrate that an EGF-responsive mammalian embryonic CNS precursor is a stem cell. *Dev. Biol.*, **175**, 1-13.

46 Appolloni, I., Calzolari, F., Corte, G., Perris, R. and Malatesta, P. (2008) Six3 controls the neural progenitor status in the murine CNS. *Cereb. Cortex*, **18**, 553-562.

47 Okada, N., Ishigami, Y., Suzuki, T., Kaneko, A., Yasui, K., Fukutomi, R. and Isemura, M. (2008) Importins and exportins in cellular differentiation. J. *Cell. Mol. Med.*, **12**, 1863-1871.

48 Perry, R.B. and Fainzilber, M. (2009) Nuclear transport factors in neuronal function. *Semin. Cell Dev. Biol.*, **20**, 600-606.

49 Yasuhara, N., Oka, M. and Yoneda, Y. (2009) The role of the nuclear transport system in cell differentiation. *Semin. Cell Dev. Biol.*, **20**, 590-599.

50 Miki, T., Takano, K. and Yoneda, Y. (2005) The role of mammalian Staufen on mRNA traffic: a view from its nucleocytoplasmic shuttling function. *Cell Struct. Funct.*, **30**, 51-56.

51 Reynolds, B.A. and Weiss, S. (1992) Generation of neurons and astrocytes from isolated cells of the adult mammalian central nervous system. Science, **255**, 1707-1710.

Downloaded from http://hmg.oxfordjournals.org/ at University of Adelaide on July 3, 2013

52 Gotz, M. and Huttner, W.B. (2005) The cell biology of neurogenesis. *Nat. Rev. Mol. Cell Biol.*, **6**, 777-788.

53 Bruno, I.G., Karam, R., Huang, L., Bhardwaj, A., Lou, C.H., Shum, E.Y., Song, H.W., Corbett, M.A., Gifford, W.D., Gecz, J. et al. (2011) Identification of a microRNA that activates gene expression by repressing nonsense-mediated RNA decay. *Mol. Cell*, **42**, 500-510.

54 Lagutin, O.V., Zhu, C.C., Kobayashi, D., Topczewski, J., Shimamura, K., Puelles, L., Russell, H.R., McKinnon, P.J., Solnica-Krezel, L. and Oliver, G. (2003) Six3 repression of Wnt signaling in the anterior neuroectoderm is essential for vertebrate forebrain development. *Genes Dev.*, **17**, 368-379.

55 Liu, W., Lagutin, O.V., Mende, M., Streit, A. and Oliver, G. (2006) Six3 activation of Pax6 expression is essential for mammalian lens induction and specification. *EMBO J.*, **25**, 5383-5395.

56 Wallis, D.E., Roessler, E., Hehr, U., Nanni, L., Wiltshire, T., Richieri-Costa, A., Gillessen-Kaesbach, G., Zackai, E.H., Rommens, J. and Muenke, M. (1999) Mutations in the homeodomain of the human SIX3 gene cause holoprosencephaly. *Nat. Genet.*, **22**, 196-198.

57 Sakurai, T. (2012) The role of NrCAM in neural development and disorders--beyond a simple glue in the brain. *Mol. Cell Neurosci.*, **49**, 351-363.

58 Kim, M., Roesener, A.P., Mendonca, P.R. and Mastick, G.S. (2011) Robo1 and Robo2 have distinct roles in pioneer longitudinal axon guidance. *Dev. Biol.*, **358**, 181-188.

59 Long, H., Sabatier, C., Ma, L., Plump, A., Yuan, W., Ornitz, D.M., Tamada, A., Murakami, F., Goodman, C.S. and Tessier-Lavigne, M. (2004) Conserved roles for Slit and Robo proteins in midline commissural axon guidance. *Neuron*, **42**, 213-223.

60 Farmer, W.T., Altick, A.L., Nural, H.F., Dugan, J.P., Kidd, T., Charron, F. and Mastick, G.S. (2008) Pioneer longitudinal axons navigate using floor plate and Slit/Robo signals. *Development*, **135**, 3643-3653.

Downloaded from http://hmg.oxfordjournals.org/ at University of Adelaide on July 3, 2013

61 Moy, S.S., Nonneman, R.J., Young, N.B., Demyanenko, G.P. and Maness, P.F. (2009) Impaired sociability and cognitive function in Nrcam-null mice. *Behav. Brain. Res.*, **205**, 123-131.

62 Bonora, E., Lamb, J.A., Barnby, G., Sykes, N., Moberly, T., Beyer, K.S., Klauck, S.M., Poustka, F., Bacchelli, E., Blasi, F. et al. (2005) Mutation screening and association analysis of six candidate genes for autism on chromosome 7q. *Eur. J. Hum. Genet.*, **13**, 198-207.

63 Marui, T., Funatogawa, I., Koishi, S., Yamamoto, K., Matsumoto, H., Hashimoto, O., Nanba, E., Nishida, H., Sugiyama, T., Kasai, K. et al. (2009) Association of the neuronal cell adhesion molecule (NRCAM) gene variants with autism. *Int. J. Neuropsychopharmacol.*, **12**, 1-10.

64 Sakurai, T., Ramoz, N., Reichert, J.G., Corwin, T.E., Kryzak, L., Smith, C.J., Silverman, J.M., Hollander, E. and Buxbaum, J.D. (2006) Association analysis of the NrCAM gene in autism and in subsets of families with severe obsessive-compulsive or self-stimulatory behaviors. *Psychiatr. Genet.*, **16**, 251-257.

65 Jolly, L.A., Taylor, V. and Wood, S.A. (2009) USP9X enhances the polarity and self-renewal of embryonic stem cell-derived neural progenitors. *Mol. Biol. Cell.*, **20**, 2015-2029.

66 Brown, C.Y., Sadlon, T., Gargett, T., Melville, E., Zhang, R., Drabsch, Y., Ling, M., Strathdee, C.A., Gonda, T.J. and Barry, S.C. (2010) Robust, reversible gene knockdown using a single lentiviral short hairpin RNA vector. *Hum. Gene Ther.*, **21**, 1005-1017.

67 Barry, S.C., Harder, B., Brzezinski, M., Flint, L.Y., Seppen, J. and Osborne, W.R. (2001) Lentivirus vectors encoding both central polypurine tract and posttranscriptional regulatory element provide enhanced transduction and transgene expression. *Hum. Gene Ther.*, **12**, 1103-1108.

68 Basak, O. and Taylor, V. (2007) Identification of self-replicating multipotent progenitors in the embryonic nervous system by high Notch activity and Hes5 expression. *Eur. J. Neurosci.*, **25**, 1006-1022.

Downloaded from http://hmg.oxfordjournals.org/ at University of Adelaide on July 3, 2013

69 Huang, L., Jolly, L.A., Willis-Owen, S., Gardner, A., Kumar, R., Douglas, E., Shoubridge, C., Wieczorek, D., Tzschach, A., Cohen, M. et al. (2012) A Noncoding, Regulatory Mutation Implicates HCFC1 in Nonsyndromic Intellectual Disability. *Am. J. Hum. Genet.*, **91**, 694-702.

70 Meinen, S., Barzaghi, P., Lin, S., Lochmuller, H. and Ruegg, M.A. (2007) Linker molecules between laminins and dystroglycan ameliorate laminin-alpha2-deficient muscular dystrophy at all disease stages. *J. Cell Biol.*, **176**, 979-993.

Downloaded from http://hmg.oxfordjournals.org/ at University of Adelaide on July 3, 2013

FIGURE LEGENDS

Figure 1. Upf3b expression during dorsal telencephalon development. A. Expression of Upf3b and related NMD and SMD factors during cortical neurogenesis. In-situ hybridisation (panels *i*) and immuno-flourescent staining (panels *ii* and *iii*) analysis of mRNA and protein localisation respectively in the dorsal telencephalon at E14.5. Bars = 100µm. Note the inverse enrichment of Upf3b mRNA and protein in the ventricular zone (VZ) and cortical plate (CP) respectively. Note inverse relationship between Upf1/Stau1 and Upf3b protein enrichment in the VZ and CP respectfully. B. Upf3b localisation within embryonic neural cells changes with differentiation and developmental time. Immunofluorescent staining of Upf3b in the developing forebrain prior to neurogenesis (Embryonic day 10.5; E10.5; bar = 20µm), during peak neurogenesis (E14.5; left panel bar = 200µm and right panel bars = 50µm) and during peak gliogenesis (E18.5; ; left panel bar=200µm and right panel bars = 50µm). Note that Upf3b is predominantly cytoplasmic in VZ progenitors at E14.5 and earlier, whilst in neurons of the CP, and E18.5 VZ progenitors, Upf3b is localised also within nuclear regions.

Figure 2. Expression of Upf3b within hippocampal neurons. A. Upf3b expression increases during neuronal growth. qRT-PCR analysis of *Upf3b* mRNA expression during the *ex-vivo* growth of hippocampal neurons and in the adult hippocampus. B. Upf3b expression is suppressed by chronic depolarisation. qRT-PCR analysis of Upf3b expression within ex-vivo cultured hippocampal neurons under physiological (5mM KCl) or depolarising (60mM KCl) conditions. *p<0.05 by Student's t-test. C. Subcellular localisation of Upf3b and related NMD and SMD factors in neuronal populations. Immuno-flourescent labelling Upf3b, Upf3a and Stau1 in hippocampal stratum pyrimidale Cornus Ammons (CA) 2 region. Upper panel bar =

Downloaded from http://hmg.oxfordjournals.org/ at University of Adelaide on July 3, 2013

100µm, lower panel bar = 50µm. Note the enrichment of Upf3b in neuronal cell bodies and nuclei, in contrast to Upf3a and Stau1 which are enriched predominantly within neurites.

Figure 3. Loss of Upf3b dependent NMD promotes the self-renewal neural stem cells. Isolated primary cortical neural progenitor cells (NPCs) were cultured normally (WT: wild type) or following transduction with Lentiviral particles encoding either inert shRNA sequences (LU: Luciferase; or S2: Scrambled T2 sequence) or one or two shRNA sequences known to target Upf3b (T2 and T5, or mixture of both (T^{2+5})). Transduced cells were purified using Fluorescent Activated Cell Sorting (FACS) to produce pure populations prior to assays. Control groups (WT, Luc and T2) and $Upf3b^{shRNA}$ groups (T2, T5 and T^{2+5}) are pooled for statistical analysis. A. Representative western-blot analysis of Upf3b protein expression. B-Actin serves as a loading control. B. Quantitation of Upf3b protein expression. C. qRT-PCR analysis of established NMD target transcripts *Snord*, *Gas5* and *Atf4*. D. MTS cell proliferation assay used to quantitate cell growth for 6 days following passage. E. Percentage of EdU labelled cells following 4 hour pulse label. F. Percentage of EdU labelled cells following release from cell cycle synchronisation in S-phase using Hydroxyurea. G. Relative percentage of sphere forming cells over 7 passages, together with average result. *$p<0.05$ students t-test.

Figure 4. Loss of Upf3b reduces the differentiation of NPCs. Neurosphere cultures of control primary cortical NPCs (non-transduced, and purified lentiviral transduced cells using particles encoding the inert shRNA sequences LU and S2) and $Upf3b^{shRNA}$ cell lines (purified lentiviral transduced cells using Upf3b specific shRNA sequences T2, T5 or combination of both) were dissociated into single cells and allowed to adhere to a substrate and cultured

Downloaded from http://hmg.oxfordjournals.org/ at University of Adelaide on July 3, 2013

further. (A and B). At day 3 of differentiation, cells were pulse labelled with EdU for 8 hours and fixed. (A) Immunofluorescent image of EdU labelled (red) transduced cells (green). Open arrows indicated unlabelled cells, closed arrow-heads indicated labelled cells. Bars = 50µm. B. Quantification of the average percentage of EdU labelled cells. C. Quantification of average colony size that result from single cells grown at very low density for 6 days. D. Immunofluorescent detection of neural cell types present in cultures at day 3 of differentiation; transduced cells (green) were stained with antibody markers against cell type specific protein markers (red; progenitor cells: Pax6; neuronal cells: βIII-tubulin; Astrocyte cells: GFAP; and oligodendrocytes (oligo): CNPase (not shown)). Bars = 50µm. E. Quantification of the percentage of progenitor cells, additive differentiated cells, and individual differentiated neural cell lineages. *p<0.05.

Figure 5. Upf3b depletion alters hippocampal neuronal outgrowth. Isolated primary hippocampal neurons were cultured normally (WT: wild type) or following transduction with Lentiviral particles encoding either an inert shRNA sequence (S2) or one of two shRNA sequences known to target Upf3b (T2 and T5). A .qRTPCR analysis of *Upf3b* mRNA expression in control (WT and S2) and Upf3b^{shRNA} (T2 and T5) neurons. Data represents average of 2 experiments (control n=4; Upf3b^{shRNA} n=4 in total). A. Representative western blot analysis of Upf3b expression in neurons from single experiment. B. Quantitation of Upf3b protein expression from the replicate experiments. C. qRT-PCR analysis of established NMD target transcripts *Snord*, *Gas5* and *Atf4*. D. Representative immunofluorescent images of control and Upf3b^{shRNA} neurons at day 5 of in-vitro growth. Bars = 100µm. Transduced cells express EGFP (Green). Cultures were co-stained using antibodies that label dendritic (MAP2; red) and axonal (TAU1; cyan) neuronal structures. E. Quantification of primary axonal length. F. Quantification of neurite termini. *p<0.05 by Student's t-test.

Downloaded from http://hmg.oxfordjournals.org/ at University of Adelaide on July 3, 2013

Figure 6. Loss of Upf3b alters the expression of alternative NMD and SMD pathways factors. Isolated primary cortical neural progenitor cells (NPCs) were cultured normally (WT: wild type) or following transduction with Lentiviral particles encoding either inert shRNA sequences (LU: Luciferase; or S2: Scrambled T2 sequence) or one or two shRNA sequences known to target Upf3b (T2 and T5, or mixture of both (T^{2+5})). Transduced cells were purified using Fluorescent Activated Cell Sorting (FACS) to produce pure populations prior to assays. Control groups (WT, Luc and T2) and $Upf3b^{shRNA}$ groups (T2, T5 and T^{2+5}) are pooled for statistical analysis of NPCs. Likewise, isolated primary hippocampal neurons were cultured normally (WT) or following transduction with S2, T2 or T5. For statistical analysis of neurons, control groups (WT and S2) and $Upf3b^{shRNA}$ (T2 and T5) were pooled, and experiments conducted in duplicate (control n=4; $Upf3b^{shRNA}$ n=4 in total). Cultures of NPCs and hippocampal neurons were analysed by either qRT-PCR or immuno-blot analysis for expression of NMD and SMD factors and targets. A-B. qRT-PCR analysis of NMD factors *Upf1*, *Upf2*, *Upf3a* and the SMD factor *Stau1* mRNA expression in (A) NPCs and (B) hippocampal neurons. (C-D) Immunoblot analysis of Upf3a and Stau1 expression in (C) NPCs and (D) hippocampal neurons. β-actin serves as a loading control. (E-F) qRT-PCR analysis of the SMD target transcripts *cJun*, *Sepine1*, *Gap43* and *Arf1* in (E) NPCs and (F) hippocampal neurons. $p<0.05$ Student t-test.

Figure 7. Validation of conserved neural targets of Upf3b dependent NMD. qRT-PCR analysis of putative UPF3B-NMD target genes *Six3*, *Mdga*, *Nrcam*, *Robo1*, *Tmod2*, and *Phgdh* in neural cells lacking Upf3b. A. Average gene expression in either pooled control NPCs (Wild-type; WT, and

Downloaded from http://hmg.oxfordjournals.org/ at University of Adelaide on July 3, 2013

control transduction NPC lines EF and S2) or pooled Upf3b knock-down NPCs (T2, T5 and T^{2+5}). B. Average gene expression experiments comparing pooled data from control neurons (WT and control transduction, EF; conducted in duplicate, control n=4) and Upf3b knock-down neurons (T2 and T5 transduced neurons; conducted in duplicate, n=4). *$p<0.05$ student t-test.

Downloaded from http://hmg.oxfordjournals.org/ at University of Adelaide on July 3, 2013

ABBREVIATIONS

CNS	central nervous system
CNV	copy number variation
EdU	5-ethynyl-2'-deoxyuridine
EJC	exon junction complex
ESC	embryonic stem cell
FACS	fluorescent activated cell sorting
HU	hydroxyurea
ID	intellectual disability
LCL	lymphoblastiod cell line
NMD	nonsense mediated mRNA decay
NPC	neural progenitor cell
PTC	premature termination codon
SBS	Staufen1 binding site
shRNA	short hairpin RNA
SMD	Staufen mediated mRNA decay
STAU1	Staufen1
uORF	upstream open reading frame
UPF3A-NMD	UPF3A dependent NMD
UPF3B-NMD	UPF3B dependent NMD
UTR	untranslated region
XLID	X-linked intellectual disability

Downloaded from http://hmg.oxfordjournals.org/ at University of Adelaide on July 3, 2013

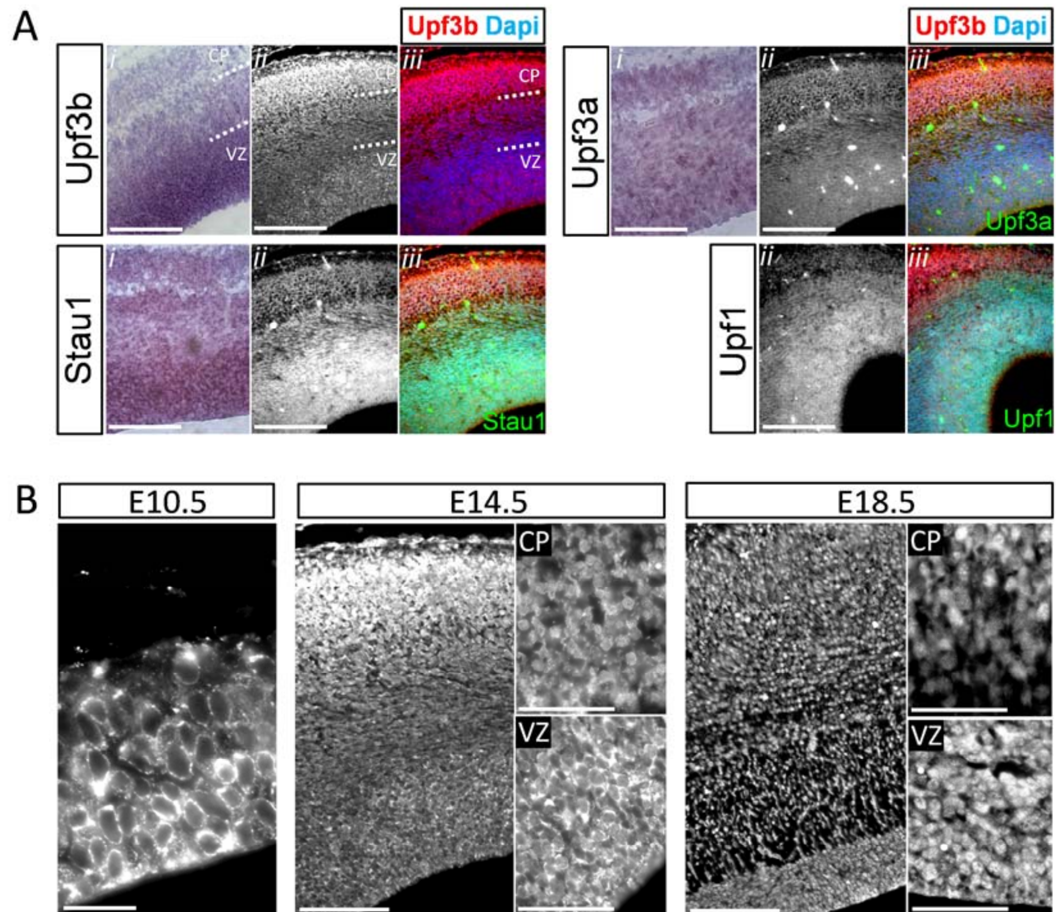

Downloaded from http://hmg.oxfordjournals.org/ at University of Adelaide on July 3, 2013

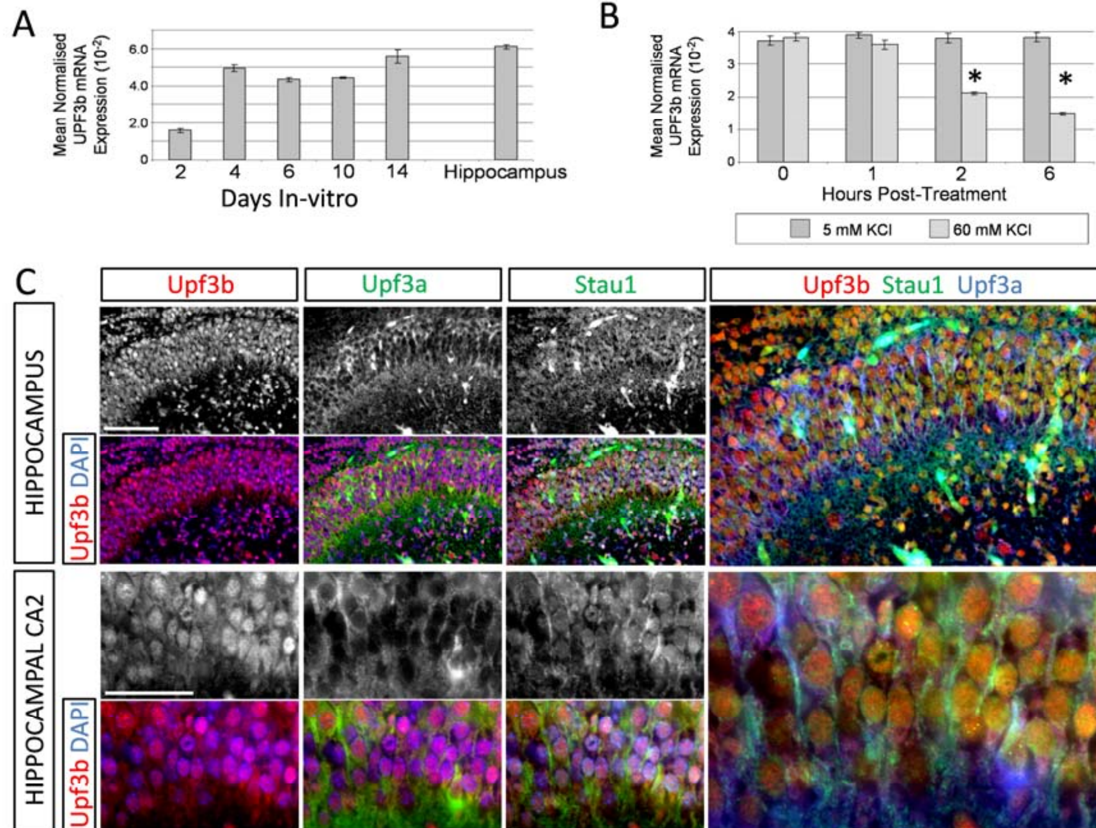

Downloaded from http://hmg.oxfordjournals.org/ at University of Adelaide on July 3, 2013

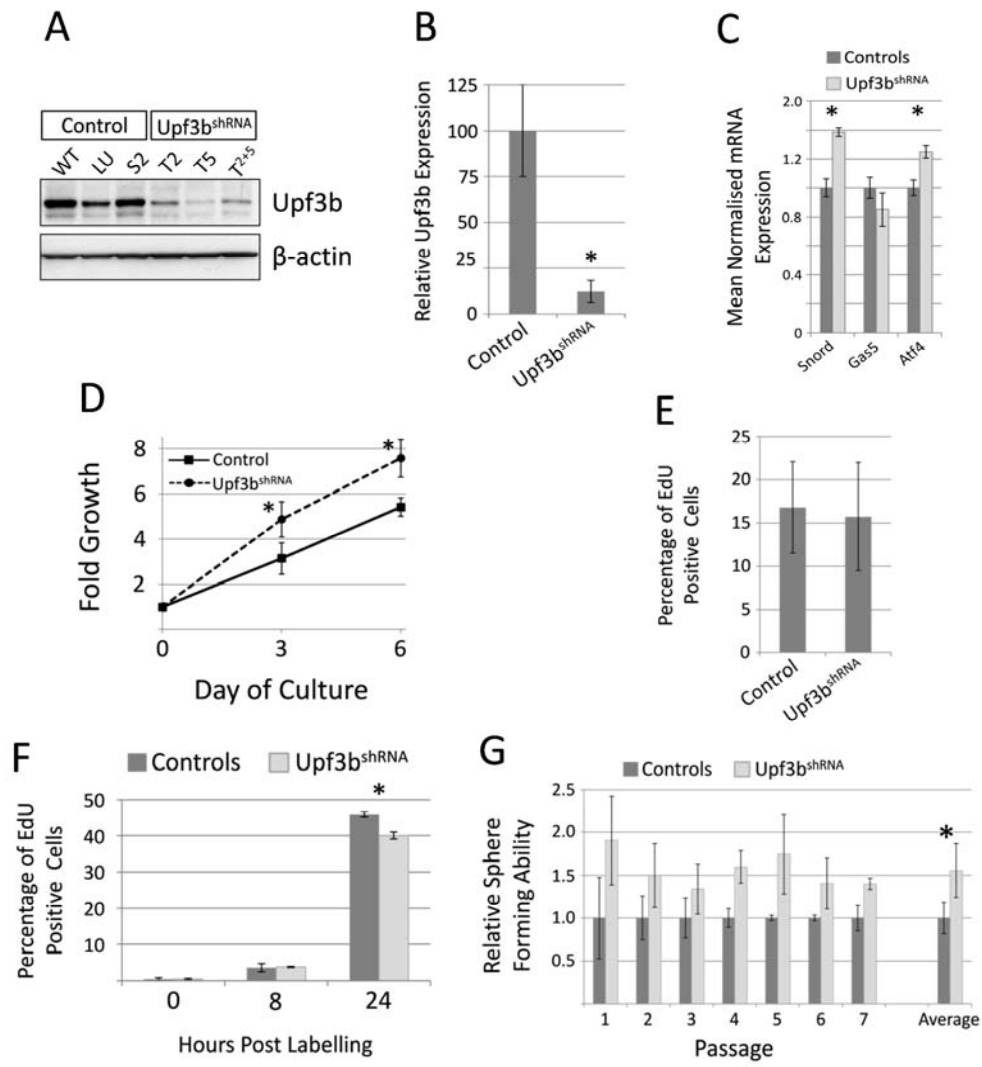

Downloaded from http://hmg.oxfordjournals.org/ at University of Adelaide on July 3, 2013

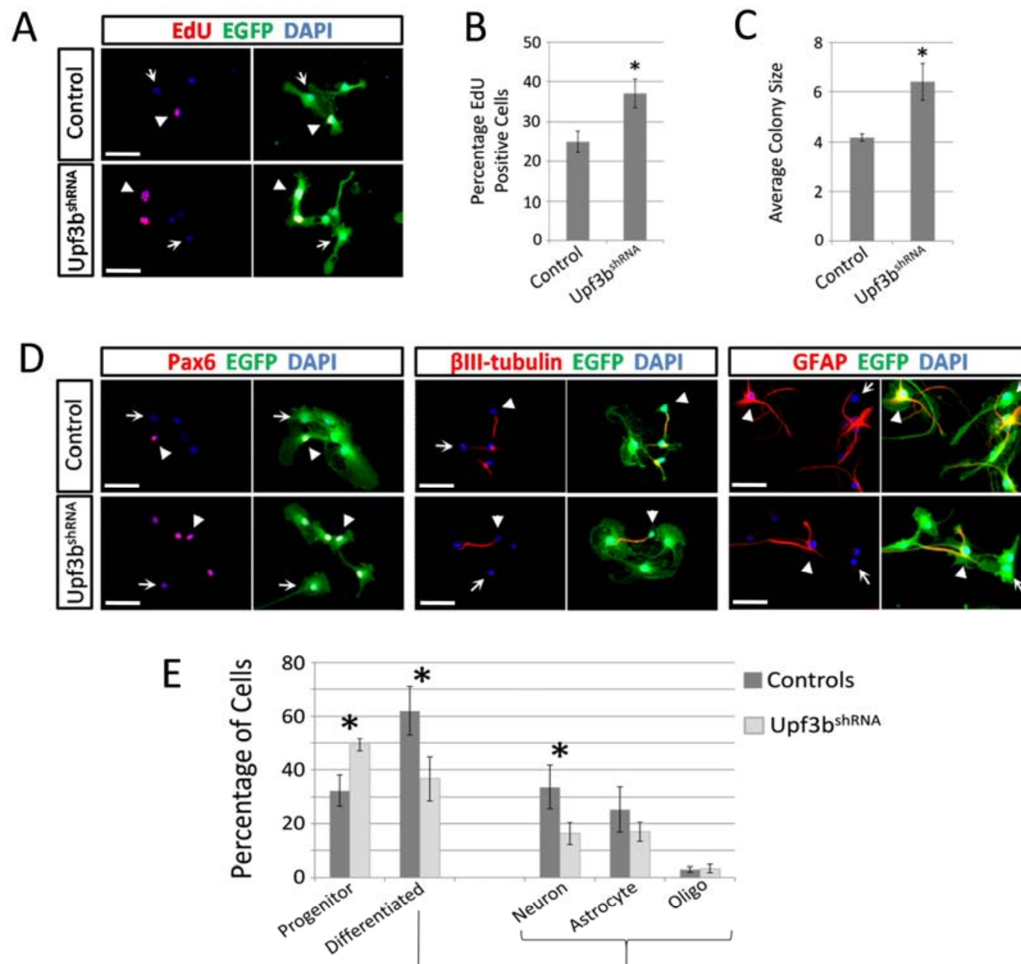

Downloaded from http://hmg.oxfordjournals.org/ at University of Adelaide on July 3, 2013

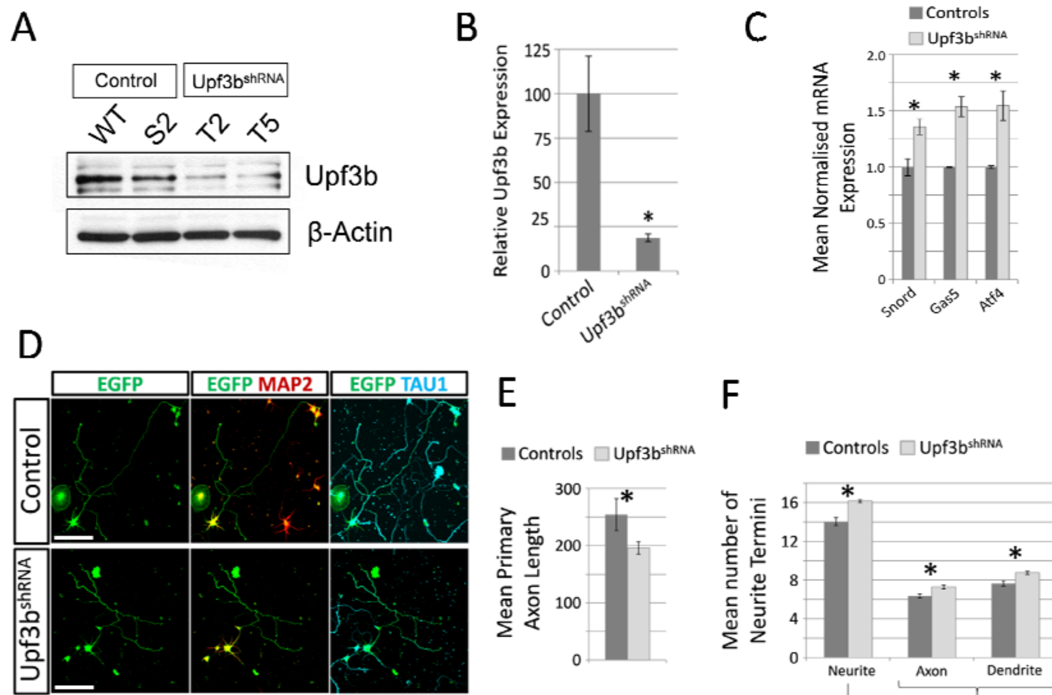

Downloaded from http://hmg.oxfordjournals.org/ at University of Adelaide on July 3, 2013

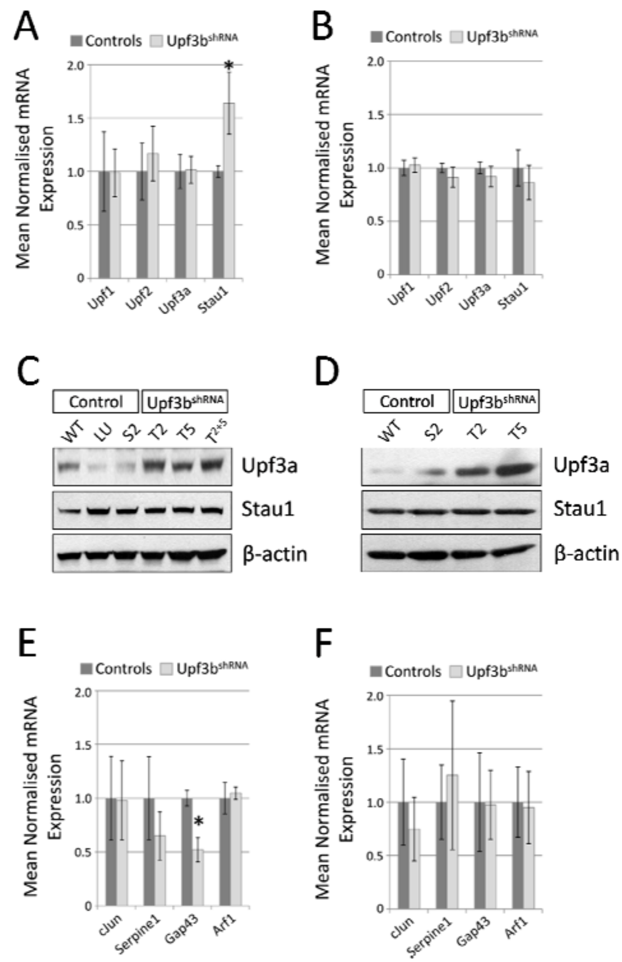

Downloaded from http://hmg.oxfordjournals.org/ at University of Adelaide on July 3, 2013

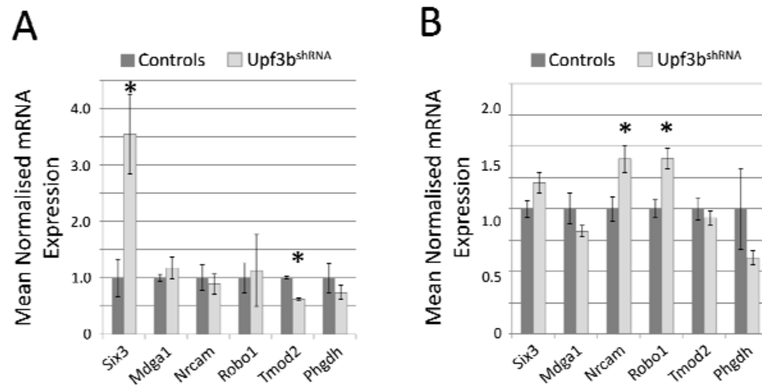

Downloaded from http://hmg.oxfordjournals.org/ at University of Adelaide on July 3, 2013